Final accepted version of Lane, S.N., Bakker, M., Gabbud, C., Micheletti, N. and Saugy, J-N, 2017. **Sediment export, transient landscape response and catchment-scale connectivity following rapid climate warming and Alpine glacier recession**. Geomorphology, 277, 210-27. https://doi.org/10.1016/j.geomorph.2016.02.015

Abstract

In the face of rapid climate warming, rapid glacier recession should lead to a marked increase in the spatial extent of the paraglacial zone in glaciated drainage basins. The extent of the paraglacial zone has been well established to be transient but there are very few studies of this transient response and what it means for sediment export. There is good reason to expect that glacier recession could increase basin-scale sediment connectivity as: sediment becomes less dependent on glacier surface transport; proglacial streams are more able to migrate laterally than subglacial streams and so access sediment for transport; and glacier debuttressing may aid the development of gullies that can dissect moraines and so aid hillslope to proglacial zone connectivity. By using records of the flushing of hydroelectric power installations we were able to develop a record of coarse sediment (sand and gravel) export from a basin with a rapidly retreating valley glacier, the Haut Glacier d'Arolla, from 1977 to 2014. Modelling suggested that these data could only be partially controlled by transport capacity implying an important role for sediment supply and potentially for the influence of changing sediment connectivity. Indeed, there was evidence of the effects of glacial debuttressing upon gullying processes and hence a possible increase in the ease of connection of upstream basins to the proglacial area. More recently, we were able to show possible temperature control on sediment export, which may only have become apparent because of the progressive development of better sediment connectivity. However, whilst rapid glacier recession should result in theory in a progressive increase in connectivity of sediment sources to the basin outlet, the supply to capacity ratio does not increase continually with glacier recession until maximum capacity is reached. We identified two possible examples of why. First, gullying was also accompanied by the sediment accumulation at the base of moraines that was too coarse to be transported by the proglacial stream, maintaining disconnection of the upper basins. Second, the sediment capacity ratio appeared to be elevated during periods of more rapid retreat and we attribute this to the importance of a continued supply of unworked glacial till before fluvial reworking and sorting of freshly exposed sediment increased the resistance of sediment to entrainment and hence export rates. Thus, the transient geomorphic response of glaciated basins to glacier recession may involve negative feedbacks that can reduce the extent to which increases in connectivity elsewhere in the basin lead to increased sediment export.

Highlights

- Presents one of the few multi-decadal records of coarse (sand and gravel) export from a glaciated river basin
- Suggests that increasing sediment transport capacity does not explain interannual variability in sediment export implying important variation in sediment supply
- Shows how connectivity develops in a glaciated basin in response to glacier recession
- Proposes that fluvial reworking of glacial till may reduce sediment transport rates and so reduce sediment connectivity

Keywords

Sediment connectivity, Glaciated, Proglacial, Sediment yield, Sediment delivery ratio

Introduction

The rapid recession of mountain glaciers in recent decades is now well documented (e.g. Barry, 2006; Fischer *et al.*, 2014). However, until recently, there have been fewer considerations of what the rapid transition from glacial to non-glacial conditions means for geomorphic processes in mountain regions (Baewert and Morche, 2014; Heckmann *et al.*, in press) despite the serious implications that this might have (Vaughan *et al.*, 2013) such as for sediment yield. The notion that glaciated basins may have substantially higher erosion rates (Koppes and Montgomery, 2009) and sediment yield per unit area (e.g. Hallet *et al.*, 1996) than non-glaciated basins is well established if debated (e.g. Hicks *et al.*, 1990; Harbor and Warburton, 1993). Given sufficient time and in the absence of other forcing (e.g. tectonic), the replacement of glacial erosion with non-glacial erosion and fluvial transport should lead to a progressive decline in sediment export rates. However, as Harbor and Warburton (1993) argued, the geomorphic complexity of such basins, including the sequential arrangement of landforms systems with different rates of sediment flux, and progressive sediment deposition and reworking (Orwin and Smart, 2004a) will make comparison of the relative contributions of glacial and nonglacial erosion to sediment yields difficult to establish.

With rapid ice cover loss, it is possible that the transient response of the landscape, at the within-basin scale and over the time scale of years to decades, dominates sediment yield, notably through the ways in which it changes sediment connectivity and so sediment flux. This transient phase has been used to label parts of the landscape as 'paraglacial' (e.g. Church and Ryder, 1972; Ballantyne, 2002, 2003) and the start of the phase may be a period when geomorphic processes are particularly efficient (e.g. Mercier *et al.*, 2009; Cossart and Fort, 2008). There are good reasons to hypothesise that this efficiency initially increases sediment yields as a result of its impact upon sediment connectivity. The net sediment export from a basin will be a function of the ease with which sediment can cascade through that system (Caine, 1976; Caine and Swanson, 1989), and so the ease with which transporting processes can connect to and transport sediment through potential sediment storage zones. Glacier recession may increase sediment connection in three ways.

First, the transition from ice cover to proglacial area should increase the level of connection between stream channels and sediment sources that have accumulated beneath a glacier. The position of stream channels under ice, and hence the sediment sources that they can access, will be limited by: (1) the ability of subglacial channels to migrate laterally by ice melt; and (2) the fact that the position of most subglacial channels is pinned by the Shreve hydraulic potential (Shreve, 1972), confirmed as a primary control on the position of many subglacial drainage systems (e.g. Sharp *et al.*, 1993; Rippin *et al.*, 2003; Evatt *et al.*, 2006; Wright *et al.*, 2008; Banwell *et al.*, 2013). Thus, glacier retreat is likely to increase the ease with which rivers can access the large amounts of erodible sediment created and stored under ice (e.g. Leggat *et al.*, 2015) and it has been shown that as long as there remains reworkable sediment within the proglacial zone, sediment flux in deglaciated zones can be maintained by fluvial activity (Warburton, 1990a; Ballantyne, 2002; Orwin and Smart, 2004a). The extent to which this effect is observed in sediment yield will, of course, depend upon the characteristics of proglacial areas themselves, such as the extent to which rapid glacier retreat is accompanied by proglacial lake formation. The latter may actually disconnect the downstream flux of glacially produced sediment (e.g. Schiefer and Gilbert, 2008; Carrivick and Tweed, 2013; Geilhausen *et al.*, 2013; Staines *et al.*, 2015; Bogen *et al.*, 2015). Indeed, it has been argued that proglacial zones may filter the signals that drive glacial sediment production (e.g. Warburton, 1990a; Harbor and Warburton, 1993; Orwin and Smart, 2004a; Geilhausen *et al.*, 2013).

Second, notably in valley glaciers, glacier recession should increase the level of connectivity between hillslopes, hillslope tributaries and the proglacial area. Material delivered by, for example, landslides, to the ice surface has a supraglacial flux that is an order of magnitude smaller than that associated with subglacial or ice marginal proglacial zones (Uhlmann *et al.*, 2013). This is not surprising given the relatively low annual surface velocities typical of many mountain valley glaciers (e.g. Mair *et al.*, 2002; Nienow *et al.*, 2005; Uhlmann *et al.*, 2013; Gabbud *et al.*, 2016). Access of glacier-delivered sediment to the subglacial hydrological system and hence fluvial sediment transport is restricted to crevasses and moulins. By comparison, sediment flux in proglacial streams has been shown to be more continual and important (e.g. Østrem, 1975; Hunter *et al.*, 1996; Lane *et al.*, 1996; Orwin and Smart, 2004a; Morche et al., 2012; Geilhausen et al., 2013; Baewert and Morche, 2014). Thus, glacier recession is likely to increase the possible connectivity of hillslope-sourced material directly to the stream network, where transport rates and hence sediment yield is likely to be more efficient.

Third, glacier recession leads to debuttressing of valley sidewalls (Porter *et al.*, 2010), and so an effective base level fall for drainage basins located above them. This should lead to headward extension of sidewall tributaries (e.g. Schiefer and Gilbert, 2007) through erosion and/or the melt of dead ice exposed to air temperatures after glacier recession (e.g. Mercier *et al.*, 2009). Sidewall streams are likely to be more efficient transporters of sediment than the hillslopes that they drain as hillslopes, notably in deglaciated environments, may have fine scale surface texture (e.g. Trevisani *et al.*, 2012) that reduces the ease of surface sediment flux. Further, evidence suggests that the legacy of past glacial activity, such as terminal moraines may disconnect glacial sedimentary systems at larger spatial scales from valley bottoms (Cossart, 2008; Cossart and Fort, 2008; Bosson *et al.*, 2015: Messenzehl *et al.*, 2014; Micheletti *et al.*, 2015b) and headward extension or gullying through such features may also facilitate the connection of hillslope-eroded sediment to the valley system.

Given the above, this paper is concerned with three broad questions. First, to consider the ensemble of these three processes, it tests the extent to which there is a marked increase in sediment export with glacier recession. Because one response to rapid glacier recession is an increase in annual water yield (at least to the point at which the relative glacial contribution to stream runoff starts to decline), it is possible that sediment transport capacity also rises. Capacity controls on transport have often been described in Alpine and glaciated river basins (e.g. Bogen, 1989; Morche *et al.*, 2008; Baewert and Morche, 2014; Staines *et al.* 2015). Thus, we quantify the extent to which, if there is an increase in sediment export, it occurs at a rate that is greater than the associated sediment transport capacity in the proglacial stream.

Second, we test the extent to which there is an evolution in sediment connectivity at the catchment scale in response to rapid valley glacier recession that might explain the relationship between changing sediment export and changing sediment transport capacity. In doing so, we aim to quantify: (1) the extent to which the expansion in size of the proglacial zone might maintain higher sediment flux; and (2) the extent to which connectivity evolves as a result of a better connection of valley side walls to the valley bottom due to the headward extension of gullies after ice mass retreat.

Third, as it is possible that the climate warming that drives glacier recession also leads to permafrost thaw and hence an increase in supply (e.g. Mercier, 2008; Bosson *et al.*, 2015; Micheletti *et al.*, 2015b), we also explore the extent to which temperature can determine variability in sediment export.

Throughout, our focus is upon coarse sediment transfer, defined as that which moves as suspended bed material or bedload as this has been traditionally harder to measure and so is less well understood. As we explain below, this has determined the focus of our work: the Haut Glacier d'Arolla, Canton Valais, south-west Switzerland (Figure 1).

Methodology

Overview

The basic goal of the methodology was to explore the extent to which evolution in coarse sediment volumes exported from a glaciated basin, during a phase of rapid glacier recession, could be related to changes in connectivity in the upstream basin. Thus, the methodology has two distinct components: (1) determination of coarse sediment export; and (2) quantification of the evolution of connectivity. These goals determined the case study chosen for the work. Not only was it important to identify a basin with an established history of glacier recession, we also needed reliable data on sediment export. The challenges of determining coarse sediment transport rates in glaciated basins even during a single melt season are well established (e.g. Warburton, 1990b; Lane *et al.*, 1996; Lane, 1997) and there are very few long term datasets on sediment export from glaciated basins (Orwin *et al.*, 2010). However, we needed export data over the timescale of decades from a basin with an established history of glacier recession and where we could isolate the effects of changing connectivity from changing sediment transport capacity. We solved this challenge in three ways.

First, we worked in collaboration with the owners of a hydroelectric power scheme (Grande Dixence SA) who have extracted almost 100% of river flow from the basin of the Haut Glacier d'Arolla, since 1962. The associated intake has to be flushed of coarse sediment periodically and from 1977 it is possible to reconstruct volumes of sediment exported. The use of purge frequency data to estimate sediment transport volumes has been reported by a number of authors (e.g. Wold and ∅strem, 1979; Lane, 1997; Bezinge *et al.*, 1989; Raymond Pralong *et al.*, 2015).

Second, we would expect that the sediment transport volume of a basin to be a function of both: (1) sediment transport capacity (i.e. hydraulic control, as conditioned by snow melt, ice melt and rain fall within the basin); and (2) sediment mobilisation and delivery. The analysis of glacial recession rates revealed a progressive increase in the annual water yield of the basin, notably from the early 1980s (Gabbud *et al.*, 2016). As this implies a progressive increase in sediment transport capacity, in order to isolate sediment supply effects and their relationship to connectivity, we developed a model for estimating sediment transport capacity based upon the volumetric coarse sediment transport model of Nitsche *et al.* (2011). We combined the sediment export volumes with the modelled transport capacity to estimate a supply-capacity ratio, i.e. inverted from the capacity-supply ratio of Soar and Thorne (2001) as it seems more logical to express sediment export as a proportion of the possible transport capacity.

Third, in order to determine controls on the supply-capacity ratio, we aimed to quantify the topographic evolution of the basin and its possible influence on connectivity, using historical digital elevation data and imagery. Messenzehl *et al.* (2014) note the dangers of relying upon morphometric analysis alone in the interpretation of how sediment connection evolves. Thus, we combine morphometric analysis with imagery but also field observations of the evolution of the basin by the first author since 1989. The morphometric and image analysis is based upon archival and specially-acquired aerial imagery, used to produce digital elevation models of the basin. These provided data on glacial recession rates (Gabbud *et al.*, 2016), including changes in the size of the proglacial area. They also allowed us to calculate the changes in the extent to which hillslopes became connected to the proglacial area as a result of glacier recession.

The Haut Glacier d'Arolla

The 12.65 km^2 catchment of the Haut Glacier d'Arolla (Figure 1) is located the Val d'Hérens, Canton Valais, in the south-western part of the Swiss Alps. The catchment includes a temperate valley glacier, with a surface area of 3.46 km^2, a mean elevation of 2987 m and a terminus altitude of 2579 m in 2010 (Fischer et al., 2014). The glacier lies primarily on a bed of unconsolidated sediments with some bedrock outcrops (Hubbard and Nienow, 1997). The wider catchment includes a number of smaller hanging glaciers, morainic material, some of which remains ice cored, rockwalls and a large and expanding proglacial area.

The glacier, as with the wider area, has been the subject of numerous scientific publications that have, together, changed our understanding of glacier dynamics and subglacial hydrology (e.g. Sharp et al. 1993; Harbor et al. 1997; Nienow et al. 1998; Swift et al. 2002; Mair et al. 2003; Willis et al. 2003; Nienow et al. 2005; Fischer et al. 2011), the relationship between glaciers and climate (e.g. Brock et al. 2000; Pellicciotti et al. 2005; Brock et al. 2006; Dadic et al. 2010) and sediment transport in proglacial streams (Bezinge *et al.*, 1989; Lane *et al.*, 1995; Lane, 1997; Swift *et al.*, 2005). The latter have shown no real evidence of outburst floods as sediment transporting agents (*cf.* Carrivick *et al.*, 2004, Carrivick, 2007) in this system.

This research aside, to date, there has been no systematic attempt to quantify the long-term evolution of coarse sediment export from the basin, nor its relationship to glacier recession and changes in hillslope connectivity. A recent study (Gabbud *et al.*, 2016) quantified the history of glacier recession over recent decades through the use of archival digital photogrammetry and provides the necessary digital elevation models (DEMs) for our analysis.

River flow data, purge frequency and estimation of purge volumes

Data on river flow for the Haut Glacier d'Arolla are available with a 15 minute resolution from 1962 and were provided to us by Hydroexploitation SA at the request of the strategic management company Alpiq Holdings Ltd. which in turn represents the owners of the scheme Grande Dixence SA. These data were used to determine purge frequency using the approach of Bezinge *et al.* (1989) who calibrated purge frequency data to determine sediment flux for the intake that is studied in this paper. The intake (Figure 1c) is part of a major hydroelectric power scheme and is designed to separate bed load and suspended load from the river discharge before the water is transferred in tunnels to a large water storage reservoir (Lac des Dix) in an adjacent valley. At present there is no requirement to leave a minimum discharge in the river downstream. Given high rates of sediment delivery to the basin, the intakes can rapidly fill with sediment and so the intakes have to be opened to flush or to 'purge' accumulated sediment and, when open, all water passes to the stream rather than being transferred to the hydroelectric power scheme. For the coarse sediment trap, gates are opened slowly over about 30 minutes. For the fine sediment trap, gates are opened over a very short period of time, typically about 30 seconds.

Before transfer, the flow has to be gauged precisely for regulatory purposes and this is done in in the fine sediment trap (Figure 1c). When either trap is flushed, the water level in the fine sediment trap reduces, very rapidly for the flushing of the fine sediment trap, more slowly for the coarse sediment trap. These draw downs need to be corrected so as to obtain a complete discharge time-series but, each correction also tells us that the trap has been emptied. Thus, the basic principle of our analysis is that it is possible to identify intake openings from the analysis of the discharge time-series as rapid drawdowns in the flow record (e.g. Figure 2).

Records were available from 1969 to 2013 with a 15 minute resolution. From 1977 to 1982, purges had already been removed from these data. Thus, for this period we use data in Bezinge *et al.* (1989). For 1983 until 2013, each purge was identified manually and removed by two individuals, one doing an initial identification and the second acting as a check. From these data, we acquired the number of purges per year and for the period 1983 to 1987, we were able to validate our method by comparison with Bezinge *et al.* (1989), which yielded a mean error of -3.9 %.

Two important steps followed once purges had been identified. First, discharge data that had been removed were then replaced by linear interpolation using values either side of the purge

(Figure 2, circles) to produce a corrected flow record. An approximation of the release flow record is then possible by subtracting the raw flow record from the corrected flow record (Figure 2, triangles) for the entire study period, but we do not use these data further in this paper. However, the corrected (1969-2013) and flow record (1983-2013) is used to model sediment transport capacity (see below).

Second, we wanted to use the purge data to estimate sediment export. The coarse sediment trap captures all fractions coarser than gravel and some sand. The sand trap is designed to allow all sediment that is maintained in suspension by turbulence to settle out before the water is transferred to a water storage lake. Thus, it is likely that all grain size fractions of sand size or greater are stored in the intake and recorded in the purge record. Up until 2007, either the gravel trap or the sand trap was purged automatically once a known sediment level was reached (Bezinge *et al.*, 1989): 100 m^3. Since 2008, automatic purging has been maintained for the fine sediment trap but operation of the coarse sediment trap has changed. For safety reasons, it was deemed preferable to purge during the night where possible (at 23h00), if the trap is filled to a certain level during the day, in addition to additional purges needed when the trap is full to 100 m^3. Thus, from 2008, the volume of each purge depends on whether it is classed as preventative or not: preventative purges have a volume between c. 60% and 100% of a full purge; others 100%. At the annual scale, this means that we have to determine a range of possible purged volumes from 2008 onwards. We did this by distinguishing between fine sediment purges (short duration, steep draw down in the flow records) from coarse purges (longer duration, slower draw down) and then adding the 60% to 100% uncertainty range to the volumes of those purges that were deemed to be coarse sediment and clear in the records at 23h00 to 23h15.

A second correction to these volumes was then needed to deal with the effects of packing density (e.g. Bezinge *et al.*, 1989; Raymond Pralong *et al.*, 2015). The model used to determine sediment transport capacity (see below) predicts the volumetric transport rate. Thus, we needed to scale our purge estimated volumes by packing density. Bezinge *et al.* (1989) reports the only field data on packing density, which was obtained by comparing volumes of sediment in the intake before and after purges with the volume of sediment deposited downstream, after flow recession. The latter is possible because the short duration of the purge leads to coarse sediment being deposited immediately downstream. They reported two values of packing density within the Val d'Hérens, for the Bas Glacier d'Arolla intake, 1,300 kgm^{-3}, and the Glacier de Tsijiore Nouve intake, 1,630 kgm^{-3}, both less that the typical values reported for gravel-bed streams (e.g. Carling and Reader, 1982). They attributed this difference to grain size effects, with the Bas Glacier d'Arolla intake accumulating coarser material. The Haut Glacier d'Arolla stream delivers material eventually to the Bas Glacier intake, so in this sense is more likely to be similar to the Bas Glacier. But the Bas Glacier is also supplied by two systems that deliver much coarser material, the Glacier de Bertol and the Glacier de Vuibe systems, which are small steep glaciated basins. Given the associated uncertainty, we treat these two packing densities as extremes and use them in the determination of error bars. To obtain volumetric packing densities, we divide the values of Bezinge *et al.* (1989) by the sediment density (2,650 kgm^{-3}) and use this to scale the purge volumes. We assume the packing densities apply equally to both coarse and fine sediment traps, which we think is appropriate because visual inspection shows that the coarse sediment trap commonly includes large amount of sand material.

The above explanation flags two sources of uncertainty in the estimation of purge volumes: (1) the effects of preventative purges; and (2) the effects of packing density. We use these uncertainties to transform the number of purges into a minimum possible volume (where we assume that all preventative purges occur with the trap 50% full and we have the Bas Glacier d'Arolla packing density) and a maximum possible volume (where we assume that all preventative purges occur with the trap full and we have the Tsijiore Nouve packing density), and so give a range of possible release volumes for each year.

Sediment transport capacity

We model sediment transport capacity using an approach that has been extensively evaluated for instrumented Swiss catchments (Nitsche et al., 2011). The approach of Nitsche *et al.* (2011) recognises that many bedload transport equations for rivers have been based upon flume experiments and, to a lesser extent, instrumented river catchments with relatively low bed slopes and relative roughness. It is argued that they tend to under-estimate energy losses associated with macroform roughness and hence over-estimate bedload flux. Whilst implicit in our paper is the recognition that such over-estimation may also come from conditions where sediment supply is insufficient to transport sediment at the capacity suggested by a bedload transport equation, we follow Nitsche *et al.* (2011) and attempt to deal with possible over prediction of bedload flux. The Nitsche *et al.* approach follows Rickenmann and Recking (2011) by developing a treatment for the additional energy losses associated with roughness elements, but where no information on the detailed spatial organization of roughness elements is available. Nitsche *et al.* found that the Rickenmann and Recking approach, even with a relatively simply representation of the effects of size selectivity on sediment transport, was preferable because of: (1) probable inadequacies in the physical representation of roughness elements in more complex treatments; and/or (2) the challenges of identifying and measuring roughness elements in the field.

Calculation of sediment transport capacity is based upon a model of: (1) flow velocity taking into account depth-dependent flow resistance; and (2) volumetric sediment transport capacity. Following Ferguson (2007), we use a variable power equation to estimate the cross-section averaged flow velocity (v_{tot}). This allows for the effects of changing flow depth upon flow resistance in a physically plausible way (Ferguson, 2007). The cross-section averaged flow velocity, including energy losses, is defined as:

$$v_{tot} = \frac{6.5(gRS)^{0.5}2.5\left(R/D_{84}\right)}{\left[6.5^2 + 2.5^2\left(R/D_{84}\right)^{1.67}\right]^{0.5}} \qquad [1]$$

where g is the gravity constant (ms^{-2}); R is the hydraulic radius (m), defined as the flow cross-sectional area divided by the wetted perimeter; S is the slope of the energy line, taken to be the mean valley slope; and D_{84} is the 84th percentile of grain-size (m). The grain-scale velocity (v_0), i.e. without energy losses, is then estimated (Nitsche *et al.*, 2011) from:

$$v_0 = 6.5\left(gRS\right)^{0.5}\left(R/D_{84}\right)^{0.167} \qquad [2]$$

Following Rickenmann and Recking (2011), [1] and [2] are combined to partition the slope (S) of the energy line into: that lost on overcoming flow resistance; and that available for sediment transport (S_0), associated with grain friction, after Meyer-Peter and Müller (1948):

$$S_0 = S\left(\frac{v_{tot}}{v_0}\right)^{1.5} \qquad [3]$$

This reduced slope is then applied to an equation for estimating volumetric sediment transport rates (Rickenmann, 1991). The volumetric transport rate per unit channel width (q_b) is given as:

$$q_b = \left(\rho_s/\rho\, g D_{50}^3\right)^{0.5} 2.5\sqrt{\theta_r}\left(\theta_r - \theta_{rc}\right) Fr \quad [4a]$$

with

$$\theta_r = \frac{RS_0}{\left(\left[\rho_s/\rho\right]-1\right) D_{50}}, \quad [4b]$$

$$\theta_{rc} = \frac{R_c S_{0c}}{\left(\left[\rho_s/\rho\right]-1\right) D_{50}} \quad [4c]$$

and where; ρ_s is the sediment density (2,650 kgm^{-3}); ρ is the water density (1000 kgm^{-3}); D_{50} is the median diameter of the bed sediment (m); θ is the dimensionless shear stress reduced through application of [3]; θ_{rc} is the reduced critical dimensionless shear stress; R_c is the hydraulic radius corresponding to the critical discharge; S_{0c} is the reduced slope corresponding to the critical discharge; and Fr is the Froude number defined as $v_{tot}/(gd)^{0.5}$, where d is the mean flow depth. Nitsche *et al.* (2011) signal the importance of reducing both the dimensionless shear stress and the critical dimensionless shear stress as [4a] is an empirical equation. The formulation in [4a] is a relatively simple threshold-based sediment entrainment formula, which does not account for processes that have been shown to be important in flume experiments (e.g. the role of a sand fraction in reducing the critical discharge necessary for sediment entrainment; Wilcock and Crowe, 2003). However, we do not have detailed information on the evolution of grain-size through time. Furthermore Nitsche *et al.* (2011) noted that this simple approach appeared to be effective in representing sediment transport provided the slope was reduced to correct for form roughness effects as per [3] on the basis of tests for a large number of instrumented Swiss catchments.

Here we estimate sediment transport capacity using slope and grain size data for the proglacial area, just before the river channel steepens and the river flows into the intake. This steeper reach, which comprises very coarse boulders, shows no evidence of sediment accumulation, and appears to be a transport reach. We use the geometry of the channel at the downstream end of the proglacial area and the value of S measured as 0.0178, at the lowest end of the range of slopes considered by Nitsche *et al.* (2011). A total of 70 samples of 100 grains gave a mean D_{50} of 0.0246 m and a mean of D_{84} of 0.0777 m. We assume that these values are representative of the bed grain size through time, although this is a source of uncertainty in our calculations.

To apply the model we take a series of water levels in increments of 0.5 mm above the minimum elevation plus 0.1 m in the section. For each water level, we calculate the number of occupied channels. For the range of possible discharges at this section, this was always one and we did not need to deal with multiple branches. The water level and cross-section morphology was then used to calculate the hydraulic radius for each branch, and [1] was applied to calculate v_{tot}. The latter was then combined with width and mean flow depth at each water level to create a look up table that allowed us to identify the parameters needed in [3] and [4] for each discharge. The model was applied by taking the corrected flow data from 1977 to 2014, matching each discharge to the look up table, and then determining the volumetric transport rate per unit width, and hence the volumetric transport rate. The volumetric transport rate was integrated through each year to get the annual volumetric transport capacity. We did not calibrate the volumetric transport capacity on the measured release volumes because we hypothesise that release volumes are a combined function of sediment supply (and degrees of sediment connectivity) and transport capacity. Rather, we calculate the supply-capacity ratio (SCR) by dividing the possible release volumes for each year by the estimated transport capacity for that year. We are also assuming some equivalence between the sediment capacity that is modelled with the Nitsche et al. (2011) approach and the sediment volumes that are stored in the intakes for eventual release. The calibration approach of Bezinge *et al.* (1989) focused on bedload transport, which is also the focus of the Nitsche *et al.* model. At the margins, in terms of suspended bedload, this might lead to some mismatch but we assume that this would predominantly shift the time-varying SCR upwards or downwards, and not change the relative variability. Although the approach makes a large number of assumptions, we emphasise that we are interested more in the relative variation in the SCR through time than in the absolute values.

Derivation of digital elevation models (DEMs), orthorectified imagery and DEMs of difference

Similar to Schiefer and Gilbert (2007), we use archival analytical photogrammetry to derive DEMs of the basin that serve two purposes: (1) they allow us to quantify the spatial patterns of erosion and deposition within the river basin; and (2) they can be used to quantify the extent to which hillslopes are connected to the proglacial stream and so able to deliver sediment. The majority of the methodology adopted is detailed in Micheletti *et al.* (2015a) and Gabbud *et al.* (2016) and only a summary is provided here. The one exception is detailed below.

Archival digital photogrammetry was used to construct Digital Elevation Models (DEMs) from 14 μm resolution historical imagery provided by the Swiss Federal Office of Topography (Swisstopo), with scales varying between 1:9,000 and 1:25,000 (Table 1). Table 1 shows the theoretical precision of elevations that might be obtained with these images (after Lane et al. 2010) given their scale and the scanning resolution used. Ground control points (GCPs), 51 in total, comprising points clearly visible on the historical imagery and that we thought might be stable over the timescale of the study were measured using dGPS survey and post-processed to the CH1903+ (Swiss) co-ordinate system. Measured points were mapped onto 0.5 m orthorectified imagery, provided by Swisstopo for 2004, to confirm that they were indeed stable. All image processing was undertaken using the Leica Photogrammetry Suite of ERDAS IMAGINE® 2008. The DEMs were derived in raster form, each in the same X Y grid, with a 1 m resolution. These results were then used to orthorectify the raw aerial images to a 0.3 m resolution.

The main difference as compared with the Gabbud *et al.* (2016) approach was the DEM analysis to determine erosion and deposition patterns. This kind of archival image analysis can cause problems because random error in the bundle adjustment phase of image processing can translate into systematic error in derived DEMs (Lane *et al.*, 2004) that becomes particularly evident when DEMs are compared. To address this problem we applied a multi-station adjustment method commonly used with terrestrial Lidar data (Gabbud *et al.*, 2015) which rotates and translates all DEMs onto a single DEM, in our case the 2009 DEM, using patches of ground thought to be stable. In our case, we identified 16 patches of ground located in zones thought to be stable across the period 1967 to 2009, each containing many 1000s of data points. The multi-station adjustment was conducted using RiSCAN PRO® (see RIEGL, 2005 for further details). Rather the multi-station adjustment automatically translated and oriented each DEM onto the 2009 DEM. Under the assumption that the patches are stable, the resultant standard deviation residuals between each DEM and the 2009 DEM, which we define as σ_{2009}, is an explicit measure of the uncertainty associated with DEM comparison (Table 1). In practice, this will over-estimate uncertainty because there may be instabilities within some of the patches used. Under the assumption that the associated residuals are normally distributed, we can assign 95% confidence limits to elevation changes as $\pm 1.96\sigma_{2009}$, the detection limit.

The DEMs and orthoimages were used in the following ways. First, we difference the DEMs and apply the detection limit to identify zones of significant erosion and deposition. Table 1 shows the detection limits and with the exception of the 1967 to 2009 adjustment comparison, the results are encouraging. The poorer results for the 1967 appear to be related to a reduction in the number of patches that can be used for comparison. We also calculate volumes of change for some regions (e.g. in the proglacial area) but note that sometimes their interpretation needs caution because if the difficulty of distinguishing between erosion and the melt out of buried ice. Second, we use the orthoimages to digitise the glacier extent on each date and we use the reduction in glacier extent as a surrogate for the increase in the proglacial area. This assumption works for the valley glacier setting here because of the steep side walls. We prefer this to digitising the proglacial area as glacier recession leaves two kinds of proglacial material: morainic material that has not been fluvially-reworked; and fluvially reworked deposits. Distinguishing precisely between these deposits is difficult on the aerial photographs, notably the older ones. However, we were able to digitise approximately the interface between fluvially-reworked and morainic material through time. Third, we derive from the DEMs parameters (e.g. slope) that aid visualisation of the evolving morphology of the proglacial area and also in an analysis of connectivity (see below).

Analysis of hillslope connectivity

Our analysis of connectivity seeks to make a distinction between process disconnection and methodological disconnection. It follows from observations made by Cavalli *et al.* (2013) that sediment connection in high mountain basins will be partially controlled by topographic roughness. A problem then arises: as the spatial resolution of the calculation of roughness becomes finer, so the determined roughness value will become progressively more influenced by noise in the DEM data. Here, we adopt a different approach, based upon one of the fundamental challenges of hydrological routing analyses.

We define process disconnection as arising when a flow path encounters a reverse slope and our aim is to quantify how this process disconnection has changed between 1967 and 2009. The extent to which this becomes an actual disconnection will depend upon the magnitude of the reverse slope and eventually, due to fill of the associated depression, the volume of fill that is possible to eliminate the reverse slope. However, it is normal practice to force flow accumulation through to the basin outlet by filling all pits that are found in the DEM under the assumption that a pit is caused by DEM noise (Arnold, 2010). We define methodological disconnection as that caused by DEM noise.

Ideally, we would be able to distinguish between these two scales of disconnection clearly, and remove methodological disconnection so as to then identify process disconnection. Such distinction is likely to be complicated for two reasons: (1) the process disconnection caused by certain landforms may be close to the threshold for methodological disconnection (e.g. a rock glacier surface); and (2) as different sub-basins have different mixes of landforms, there may be little possibility of generalising the distinction at the landscape scale. It is only possible by reference to the landforms that make up the sub-basin being considered. Hence, an important step in the analysis is to simulate how, for different sub-basins, changing the threshold assumed to be methodological disconnection impacts flow paths and hence flow accumulation.

We do this through quantifying the effect of different levels of DEM filling on the area upstream contributing to the main valley (A). The approach follows from Peñuela *et al.* (2015) who considered overland flow connectivity as a function of when a critical level of depression storage is reached. Here, we conceptualise the problem in the same way, by considering how connectivity changes as pits are progressively filled. At low levels of fill, we would expect A to not change much. As we approach the level of likely noise in the DEM, we would expect A to increase rapidly until the level of fill at which noise has been completely removed and *A* no longer increases. That is, we would expect the relationship between *A* and the level of fill to take the form of an ogive. However, in the presence of process disconnection, we would expect this transition to occur at greater levels of fill, with the delay being a function of the kind of landform responsible for the process disconnection. The length scale at which the ogive becomes asymptotic then defines the level of process disconnection along the flow path. Thus, in a first exercise, we quantify the response of *A* to a progressive increase in the level of DEM fill. We begin by filling all depressions less than 0.1 m and we quantify *A*. Then, we double the fill progressively until the maximum considered, 102.4 m.

In order to calculate *A* we need a flow routing algorithm and we use Holmgren (1994) where:

$$FS(i) = \frac{\left(\tan\beta_i\right)^x}{\sum_{i=1}^{8}\left(\tan\beta_i\right)^x} \quad [5]$$

and β_i = slope in direction *i* ; *FS(i)* = proportion of flow going in direction (*i*) ; *x* = a parameter that can vary between zero and infinity. As *x* tends to infinity, FS tends to route all the flow in a single direction, that is the line of steepest slope (commonly known as a D8 algorithm). For *x* = 1, flow is routed evenly in proportion to slope. For *x* = 0, flow is routed equally between all cells regardless of slope. As we do not wish to impose a value of *x a priori*, we undertake the exercise of progressively filling the DEM for a dyadic series of *x* = 1; 2; 4; 8; 16; and 32. The pit filling and flow routing uses the DEM analysis tools in the TopoToolBox of Schwanghart and Kuhn (2010).

We interpret these results with respect to four sub basins on the east side of the valley that in total, under perfect connection, could supply 10.8% of the total basin area. For each area we plot the logarithm of the accumulation area that results with each level of DEM fill, and for each value of the parameter *x* in [5]. We interpret these plots in two ways. First, for each sub basin, we compare the spatial scale at which perfect connection is reached (i.e. the maximum possible accumulation area), for 1967 and 2009. We choose these two dates as an end member comparison. Second, we consider the change in sensitivity of the calculations of accumulation area to the parameter *x* for 1967 and 2009. We hypothesise that with incision and headward extension of gullies, the sensitivity of accumulation area to *x* should decrease.

Results

Sediment transport capacity, sediment export and the supply-capacity ratio

Figure 3 shows the modelled annual volumetric transport capacity from 1968 to 2014, with the measured basin water yield superimposed. Both increase as a function of time. The relative rate of increase, defined as $\left(\bar{t}/\bar{x}\right)\left(dx/dt\right)$, where dx/dt is the linear rate of change of *x* (capacity or yield) as a function of *t* (time), is greater for the capacity ($\left(\bar{t}/\bar{x}\right)\left(dx/dt\right)$ = 21.7) than it is for the yield ($\left(\bar{t}/\bar{x}\right)\left(dx/dt\right)$ = 16.9): the capacity increases at a greater rate than the yield. Given the form of [4], it suggests that there is a greater duration of excess shear stress over its critical value due to more extreme river flows. This may be achieved through either progressively greater glacier melt volumes or systematic change through time in the extent to which the subglacial drainage system is more channelised and so producing flow hydrographs with better defined peaks (e.g. Nienow *et al.*, 1998). The water yield is more strongly correlated with time (0.703, $p < 0.001$) than the transport capacity (0.589, $p < 0.01$), which may be due to greater interannual variability in the efficiency of the subglacial drainage system than in the volume of snow and ice melt. However, annual water yield and annual transport capacity are strongly correlated (0.950, $p < 0.001$) which is not surprising given the form of [4]. There is some temporal variability in both water yield and transport capacity during the 1970s and this reflects wider observations of a cooler snowier period leading to greater snow accumulation in this region during the late 1970s (e.g. Micheletti *et al.*, 2015b; Gabbud *et al.*, 2016).

Figure 4 shows the modelled annual volumetric transport capacity and the export volume estimated from the records of intake flushing. The latter show some increase in uncertainty from 2008, when the intake operation was changed to automatically flush if the basin was at least 50% full, during the night. Sediment export is relatively low from 1976 to 1980 after which it becomes higher but variable to 1994. It then becomes low again until 2003. As a result, whilst there is a significant correlation between capacity and export ($r = 0.415$, $p < 0.02$), transport capacity only explains c. 17% of the variability in sediment export.

Figure 5a shows the supply to capacity ratio (SCR) and reflects the data in Figure 4. First, the SCR is uniformly less than one (implying less export than transport capacity). Although the precise values of the SCR will be influenced by uncertainties in the estimation of the annual transport capacity, as values greater than 1 are implausible, Figure 5a suggests that the relative variability in the SCR are plausible. Second, standardisation of the export by the capacity to create the SCR still does not produce a record of progressively increasing SCR that we hypothesised would follow from glacier recession and the progressive increase in connectivity. It seems that for the period 1977 to 1980, there are low values of SCR (compare Figure 4 and 5a), they then rise and are variable to the mid 1980s, and then decline to 2002 (1992 being a notable exception). From 2002 to 2011 there is a consistent rise, before again a decline in the most recent years.

Relationship between the supply-capacity ratio, glacier recession and the development of the proglacial area

On the basis of Figures 4 and 5a, it appears that there is some decoupling of the relationship between annual transport capacity and sediment export within this system. Figure 5a shows the cumulative area of proglacial zone exposed due to glacier recession. Whilst the area increases continuously, the SCR does not. However, the two periods of rising SCR have more rapid increases in proglacial area than the period in between when the SCR is falling. There may be some relationship between the SCR and the rate of glacier recession but this is difficult to elucidate with the resolution of aerial imagery available.

Figure 5b shows the mean annual temperature on a south facing terrace (Bricola, Val de Ferpècle) at an altitude (2'430 m) only slightly lower than that of the Haut Glacier d'Arolla terminus (2'600 m) and 7.8 km to the North North-East. Whilst there appears to be a negative relationship between the supply-capacity ratio and temperature until about 2000 ($r = -0.508$ $p < 0.05$), from 2000 there is a significant positive correlation ($r = 0.714$, $p < 0.01$). The same occurs with the relationship between sediment export and temperature (Figure 5b), with a correlation of -0.385 ($p < 0.05$) to 2000 and 0.821 ($p < 0.001$) from 2000. As the glacier retreats, there is evidence of the onset of temperature forcing.

Following the observation of Marren and Toomath (2014), it is important to interpret these patterns in the context of a more detailed evolution of the proglacial area. Glacier recession does not necessarily just leave a proglacial stream, but also morainic material and related features which may constrain the ability of the stream to access and to transport poorly consolidated sediment. Thus, Figure 6 shows the evolution of the proglacial area from 1967 to 2009. In 1967 (Figure 6a) there was a very small proglacial area. The glacier terminus was oriented diagonally across the valley reflecting steeper slopes on the west side of the valley which leads to shading and slow melt rates. Between 1967 and 1977 (Figure 6b) there was terminus retreat of approximately 300 m on the east side of the valley to create a narrow corridor of proglacial stream bounded by ice to the west. This process continued to 1983 (Figure 6c) albeit somewhat more slowly and also with some evidence of advance of the west side of the terminus. From 1983 to 1988 (Figure 6d) terminus recession and expansion of the proglacial area remains slow. From 1988 to 1997 (Figure 6e) there is some widening of the proglacial area and also some further snout recession but this is over an 11 year period and so is relatively slow. When taking into account the shorter duration, there is a marked recession to 2000 (Figure 6f), with widening of the proglacial area. Retreat and widening continue to 2005 (Figure 6g) and then 2009 (Figure 6h). Broadly speaking, these patterns reflect the quantitative data regarding the increase in the proglacial area (Figure 5). Closer inspection of the imagery, plus field observations, do counter this observation slightly because within the growing proglacial area there was evidence of ice-cored moraines. Figure 7 shows slope maps for the proglacial zone in 1997 and 2009, showing how a large zone of ice cored moraine melted out leading to a substantial increase in the width of the proglacial area.

Erosion and deposition in the proglacial area

Figure 8 shows the mean surface changes per year for the periods when data are available for zones that are fluvially reworked according to the most recent aerial image. The date at which they become fluvially reworked is taken as the start date of the first period for which surface change can be calculated. In most but not all cases, this start date is also the first date when the glacier appears to have retreated through the identified area. This is not always the case, however, because reworking by the river can be limited by the melt out of ice cored moraine. For instance, Figure 8a shows areas labelled as 2005 and 2009 but surrounded by earlier dates. This corresponds to the zone of ice-cored moraine flagged in Figure 7 that had only melted out by 2009.

Up until the 2000-2005 period, the proglacial zone progressively lowers in all cases (Figure 8b). There are two explanations for this. First it may be due to evacuation of accumulated sediment by the river. Figure 6h shows that most of the proglacial stream is braided and with ice retreat, such that the stream is no longer pinned by the hydraulic potential of the ice mass, the area of sediment that the stream can erode should go up. Second, it is not possible to distinguish this effect from the ongoing melt of ice-cored till. For the period 2000 to 2005, all areas undergo fill, with two of these areas also filling between 2005 and 2009. The effect of this change is that there appears to be a positive slope in Figure 8b. It may suggest that the proglacial stream is switching from being dominated by: (a) surface lowering to ice melt and fluvial erosion, with implications for fluvial sorting of sediment; to (b) surface rise associated with sediment deposition.

Hillslope connectivity and evolution

Figure 9 shows the flow accumulation area calculated for 2009 along with the glacier margin in 1967 and 2005 calculated with all pits filled. In a general sense, it emphasises the potential importance in this kind of environment of the heritage of previous glacial activity. Above the 1967 line (to the north-east on Figure 9) there is a clear rupture in the flow accumulation area that corresponds to the ridge of the Little Ice Age moraine dating from the mid 1850s. Thus upstream basins have the potential to be highly disconnected. Figure 9 also shows that the incised streams, that are now apparent in the steep deglaciated zone between the 1850s moraine and the proglacial area, have the potential to become disconnected where they join the proglacial area: they become distributary systems. Field observations suggest that this relates to the accumulation of very coarse material (> 0.5 m diameter) at the bottom of the hillslopes that cannot be transported by the proglacial stream even under extreme conditions.

Figure 10 shows the evolution of the relationship between upslope contributing area for different levels of DEM fill for 1967 and 2009, for the four sub basins shown on Figure 9. Two sub basins

(1 and 2) were located down valley of the glacier terminus in 1967 and two were located between the 1967 and 2005 positions of the glacier terminus (Figure 9). As expected, in all cases, the upslope contributing area increases with the level of DEM fill. In 2009, for the two smallest sub basins (2 and 3), there is very little evolution of basin area with fill, suggesting that these are generally well connected basins on this date. For the two larger sub basins (1) and (4) there is some evolution with connection being achieved in basin (1) at around 0.8 m and basin 4 at around 1.6 m. These values can be compared with DEM related noise as suggested by either the RMSE z or the $1.96\sigma_{2009}$ (Table 1). If we take the more conservative measures suggested by $1.96\sigma_{2009}$, then the critical level of fill for sub basin 1 is close to DEM noise, but the value for sub basin 4 is somewhat greater. There remains some process disconnection in sub basin 4.

More interesting is the evolution in the levels of fill needed to achieve connection when 1967 and 2009 are compared (Figure 10). Higher levels of fill are required to get the maximum values of accumulation area for three sub basins: 3.2 m for sub basins 1 and 3; and 6.4 m for sub basin 4. Table 1 suggests that there is greater uncertainty in the 1967 elevation data. However, this is only in the $1.96\sigma_{2009}$ estimate and may be as much to do with difficulties in identifying patches for the rotation and translation of DEMs as the elevations themselves, especially given that the DEM analysis that we are undertaking here will be more dependent on local, relative elevation variability than absolute georeferencing. Further there does not appear to be noise present that effects connection in sub basin 2. Thus, we tentatively conclude that there appears to be higher levels of disconnection in 1967 than in 2014, and higher levels of disconnection for those sub basins where there has been more recent terminus retreat (sub basins 3 and 4).

Greater confidence in these conclusions is obtained by considering erosion and deposition patterns between 1967 and 2009. Figure 11 shows erosion and deposition on the east side of the glacier for four periods and this includes sub basin 4. The glacier itself can be seen as zones of lower slope (< 0.3) in Figures 11e through 11h. In 1983 (Figure 11e) there is a clear line of contact (co-ordinates [2'400, 2'000] to [2'850, 1'400]) between glacier ice and the sidewall but with a terrace most likely comprising ice-cored till to the right of this contact line. Figure 11a shows extensive surface lowering of the main glacier and the terrace between 1967 and 1983 but also some sediment accumulation where ice at the base of the slope can act as a base level control and aid the accumulation of sediment delivered by gravitational processes. General surface lowering continues throughout the hillslope between 1983 and 1988 (Figure 11b), more rapidly in the terrace zone than in other parts of the sidewalls. By 1997, gullying of the sidewalls is clear in a number of places shown in both the slope map (Figure 11g, linear features, orthogonal to the glacier margin with slope values approaching 1) and also the DEM of difference (Figure 11c). The development of one such gully can be seen in the aerial imagery by comparing Figures 6d and 6e, the left of the three gullies that appear in the bounding box on Figure 6e. These processes continue between 1997 and 2009 (Figure 11d). Figure 12 shows the development of these three gullies in section from 1983 to 2009, showing that incision has occurred to greater than 10 m in depth. Note that the incision in the sub basin 4 gully (to the left) is lower. Those to the right drain sub basins that are not considered in this analysis because the DEM for 2009 does not quite extend to include their full catchment extents. Thus, the accumulation areas shown for them in Figure 9 are lower than the correct ones.

Discussion

Rapid glacier recession and sediment yield

The focus of this paper is a glacier that has undergone near continual recession in terms of its loss of surface area and the associated increase in the area of its proglacial zone (Figure 5). This rapid recession is widely reported for the European Alps and, for instance, glaciers in Switzerland have lost one third of their area since 1973 (Fischer *et al.*, 2015). Studies of what this might mean for sediment yield are much rarer and have tended to make the assumption that sediment yield is a function of transport capacity.

Figure 3 shows a progressive rise in water yield and the associated sediment transport capacity for the Haut Glacier d'Arolla basin from 1968. The rising water yield is likely to be primarily a temperature signal. Micheletti *et al.* (2015b) synthesised data for this region and observed that aside from a wetter period in the late 1970s and early 1980s, total precipitation has generally remained stable or declined weakly. Basic snow depth modelling (Micheletti *et al.*, 2015b, Figure 5) suggested a progressive decline in the accumulated March snow depth from the early 1980s of about 40% at an altitude of 2'500 m; with also very low levels of snow remaining in the glaciated parts of the basin at the end of the ablation season (September). Thus, rising yield appears to be more closely related to temperature rise, and increasing glacier melt, than precipitation or snow effects and annual water yield and mean annual temperature are significantly correlated (r = 0.547; p < 0.01). Sediment transport capacity is not significantly correlated with temperature (r = 0.290; p > 0.05) neither globally, nor in the period from 2000 when temperature correlates with the supply-capacity ratio (Figure 5b). This points to the important control of the non-linear form of [4] such that estimated sediment transport capacity is restricted to a smaller percentage of the year than water yield, as illustrated for an example year (2014, Figure 13). Under the assumption that [4] and its application are valid, the capacity of the proglacial area to transport sediment has some potential to act as a control on sediment export. Sediment transport capacity and sediment export were significantly correlated (r = 0.415, p < 0.01) and we can conclude that sediment transport capacity is at least in part a control of sediment connectivity in the system (*cf.* Hooke, 2003).

That said, this correlation means that only about 17% of the variability in sediment export is explained by the estimated sediment transport capacity and this is confirmed in Figure 4. Notably, from the early 1990s until the early 2000s, whilst estimated transport capacity continues to rise, sediment export falls to very low levels. This is shown clearly in the supply-capacity ratio (Figure 5) and the SCR variability may be related to three controls on disconnection, each related to transport capacity: (1) a non-linear relationship between spatial scale and transport capacity; (2) sediment sorting processes which reduce transport capacity; and (3) legacy controls on the river channel access to erodible sediment.

First, even in a basin that was not glaciated, we would expect sediment transport capacity to decrease more rapidly with distance upstream because sediment transport capacity is a non-linear function of excess shear stress over a critical value, that is there is a minimum upstream area needed, in combination with local bed slope, before transport can begin. This will be reinforced in a glaciated basin because the possible sources of water are not distributed in the same way as in a non-glaciated basin, they are concentrated in glaciated parts of the basin, so reinforcing the spatial variability in transport capacity. Thus, disconnection can occur because the transport capacity does not downscale linearly.

Second, Figure 5 suggests that as the glacier recession slowed from the late 1980s to the late 1990s, so the supply-capacity ratio declined. Albeit with perhaps a small lag, which may be as much due to the temporal resolution of the aerial imagery as it may be due to a process effect, when the glacier recession rate begins to rise, the supply-capacity ratio follows. Thus, whilst glacial recession appears to replace ice constrained streams with streams that are much freer to migrate, this does not transfer into a progressive increase in sediment yield. One theory to explain this observation is that fluvial sorting of sediment progressively increases the resistance to motion of proglacial stream channels once ice has retreated. It is well established that fluvial sediment transport leads to sediment sorting (e.g. Bacchi *et al.*, 2014) including in mountain (e.g. Bacchi *et al.*, 2014) and proglacial streams (e.g. Ashworth *et al.*, 1992; Kociuba and Janicki, 2015). Indeed, glacier recession commonly leads to initial stream incision (Marren and Toomath, 2014), something that would aid the sorting process. In our case, there is evidence of incision after initial glacier recession (Figure 8b) but this cannot be distinguished from the effects of melt out of ice cored till. As glacial till is commonly poorly sorted (e.g. Santos-Gonzalez *et al.*, 2013), glacier recession leads to the exposure of poorly sorted sediment. This leads to increased sediment supply but only in so far as it is not countered by increases in the resistance of sediment to entrainment due to subsequent fluvial sediment sorting. Following Church and Ryder (1972), sediment sorting becomes an early contributor to declining sediment yields during the period when the extent of paraglacial sedimentation is important. Orwin and Smart (2004b) observed how overland flow effectively armours till, making it more resistant to erosion. Here, we propose it may also apply to fluvially-reworked sediments. It points to a weakness in our use and application of [4] as the decline in the supply-capacity ratio may be due to our failure to allow for the critical entrainment threshold to rise due to fluvial reworking of sediment, and hence the sediment transport capacity to fall. In process terms, it further implies that sediment transport capacity is an ultimate control upon the connection of proglacially stored sediment to the basin outlet. Maintaining high sediment supply to the basin outlet is dependent upon a rate of glacier recession and supply of poorly sorted till that is greater than the rate at which the proglacial stream can sort it, unless there are extreme flood events capable of mobilising well sorted fluvial deposits. The importance of extreme floods as a control on total sediment yield in proglacial streams has been observed (e.g. Warburton, 1990b; Nicholas and Sambrook-Smith, 1998; Lamoureux, 2002; Kociuba and Janicki, 2014).

Third, despite rapid glacier recession, there is evidence that the active channel zone remains constrained by the legacy of glacial occupation: glacier recession does not necessarily lead to an expansion in proglacial stream width, and hence the width of the deposit that the stream is able to access. Figure 7 showed how a zone that was deglaciated by the mid 1990s still has substantial ice cored moraine that had only melted out by 2009. Marren and Toomath (2014) observed that such moraines may serve to limit the lateral erosion by the stream channel and so the width of the proglacial area available for the river to access sediment.

In summary, our data suggest that there may be an association between glacier recession and sediment export but that this may only be a transient response. Inherently, sediment transport capacity will remain limited by a non-linear relationship with spatial scale. Whilst glacier recession does increase the ease with which stream channels may connect to potentially transportable sediment, this connection may initially be limited by ice-cored moraine and till. Further, fluvial reworking of till material may serve to increase entrainment thresholds and so reduce sediment flux to the basin outlet. Such increases do not disconnect potential in-channel sediment sources permanently. Rather they make them reliant upon extreme sediment transport events. The work emphasises that hydraulically-based bedload transport equations such as [4] should not be used as a means of estimating sediment export from these kinds of basins, even after calibration, as it appears that export is controlled strongly by supply limitation (see also Stott, 2002).

Hillslope sediment connectivity and its impact on sediment export

The initial evaluation of sediment connectivity (Figure 9) showed the important potential of past glacial activity upon the landscape and, in theory, the decoupling of hillslope-derived sediment. For instance, it was possible to identify clearly the effects of a Little Ice Age moraine ridge on flow routing and sediment disconnection as others have observed (e.g. Cossart, 2008, Cossart and Fort, 2008). Sediment connection by water can only be achieved once the ridge has been breached.

Figure 9 identified two basins that were inside the terminus in 1967. For the basin farthest upstream it was possible to identify the progressive development of gullying into the Little Ice Age moraine (Figure 12) that will have served to aid this connection. Curry *et al.* (2006) described this process in a similar Alpine setting, noting that gullying tended to develop over about 50 years from deglaciation after which gully relief reduced due to gully infilling. The DEMs of difference (Figure 11) did suggest some deposition on these slopes that we attributed to sediment falling from higher altitudes on the moraine, notably before glacier retreat when there was a higher base level. However, there was no evidence of gully infilling suggesting that these gullies are still in a phase of incision. This incision occurred in parallel with continued ice melt out but at a faster rate such that gullies were clearly evident in the topography (e.g. slope, Figure 11; sections, Figure 12) at the end of the period. Without this incision, it is likely that the Little Ice Age moraine would act as a sediment sink (Bosson *et al.*, 2015), disconnecting the upper basins shown in Figure 9 from the proglacial area of the Haut Glacier d'Arolla

We aimed to see if it was possible to quantify an evolution in hillslope connectivity ('process disconnection') in response to glacier recession. We made the assumption that the primary process of sediment transfer is hydrological and so focused upon the analysis of hydrological flow paths on two dates, 1967 and 2009. As one of the basic problems of flow path analysis is that hydrologists have traditionally forced perfect connection upon landscapes in the calculation of accumulated area and given the possibility of noise in the older datasets used ('methodological' disconnection'), we explored how the level of connectivity as represented by flow accumulation area changed with the level of pit filling applied to the data. This is a new way of considering the uncertain relationship between methodological and process disconnection. By considering four basins, two of which had been subject to a much shorter period since glacial debuttressing, we found that there was some evolution in connected upslope areas: perfect connection was found to occur at lower levels of DEM fill for: (1) those sub basins debuttressed for longer; and (2) in 2009 data as compared with 1967 data. In addition, there was some evidence of reduced sensitivity to the diffusion parameter in [5] in the 2009 data which may suggest a surface that is more incised. It appears that there has been an evolution of hillslope connectivity at least in the hydrological terms implicit in this kind of DEM analysis. That said, it was evident that the Little Ice Age moraine had already been breached in some locations by 1967. Thus, the period of study represents a period of developing connectivity that, with progressive glacial debuttressing and gully development, both of the Little Ice Age moraine and at higher altitudes within the sub-basin, rather than the onset of connectivity that was not there before. Further, the development of greater levels of upstream connectivity may not have been sufficient to connect these upper basins. Figure 9 shows that as the moraine gullies approach the proglacial area, the flows become more diffusive as they encounter very coarse material that accumulates at the toe of the moraine. This material is hard to erode and whilst there may be some throughput of suspended material, field observations suggest that these could be zones of deposition and sediment accumulation, reducing sediment flux to the zone of fluvial reworking. It is not yet completely clear that these higher sub basins are evolving to the point at which they can contribute significantly to exported sediment.

There is one counter to this observation in the results in Figure 5b. This shows that a very strong association between mean annual air temperature and sediment export occurs from the early 2000s (r = 0.821, p < 0.001). This was accompanied by a reversal in the correlation between temperature and supply-capacity ratio that was negative to 2000 (r = -0.508, p < 0.05) and then positive from 2000 (r = 0.714, p < 0.01). The negative correlation between temperature and supply-capacity ratio could be explained by a system where sediment supply does not respond as much to climate forcing as melt and hence transport capacity. The positive correlation suggests a system where sediment supply responds more sensitively to climate forcing than does capacity. To remove the possible effects of temperature on capacity and so to isolate the direct effects of temperature on sediment export, we calculated the partial correlation between temperature and export, taking into account capacity variability. There was no significant correlation between export and temperature until the 2000s (r = -0.465, p > 0.05) but a highly significant relationship between export and temperature afterwards (r = 0.812, p < 0.001). This shift in pattern may reflect direct temperature effects on permafrost melt and sediment production on the hillslopes. Although the processes involved are complex (Huggel *et* *al.*, 2012; Stoffel and Huggel, 2012), the potential importance of permafrost degradation for sediment flux has been observed in similar Alpine settings (e.g. Chiarle *et al.*, 2007; Kniessel *et al.*, 2007; Lugon and Stoffel, 2010; Bennett *et al.*, 2013). It is possible that given the hypsometric curve of this basin, the mean annual average temperatures are such that the altitudes of possible permafrost degradation have increased since 2000 to capture zones of previously accumulated but frozen sediment. Given the apparent evolution of basin connectivity (e.g. Figure 10), such material is increasingly delivered to the proglacial area. For the latter to occur, there has to have been sufficient retreat of the main glacier, to avoid material accumulating in ice marginal zones. Thus, the results in Figure 5b may be the result of the evolution of connectivity between hillslopes and the proglacial area, following main glacier recession such that, since 2000, sediment production due to permafrost degradation becomes the limiting control on total sediment export. This observation may emphasise why linkages between permafrost degradation and sediment export from basins are complex. It also suggests that high frequency records of sedimentation (e.g. in proglacial lakes) will only reflect climate drivers in so far as sediment delivery is not limited by connectivity (Micheletti *et al.*, 2015b).

Synthesis

Figure 14 attempts to synthesise the above discussion in a way that emphasises the established importance of the sediment cascade in this kind of environment (e.g. Slaymaker *et al.*, 2003; Morche *et al.*, 2008; Otto *et al.*, 2009; Bennett *et al.*, 2014; Messenzehl *et al.*, 2014). The presence of a systematic variation in sediment export can be traced to the transient response of the system to rapid glacier recession. This may be direct, such as through the ways in which glacier recession replaces slower glacier surface sediment transport with more rapid fluvial transport; or through the greater freedom of the proglacial stream to access sediment as compared with subglacial channels. But it also occurs indirectly through the evolution of landscape connectivity associated with processes like glacial debuttressing. Connectivity is clearly dynamic. Its evolution may explain the onset of temperature forcing of sediment export as higher levels of connectivity are established that connect respective sediment sources to the channel network.

However, the evolution of this connectivity can both increase and decrease the strength of coupling between components of the landscape. Although further data collection and analysis is needed to confirm the conclusion, provisional results suggest that whilst the initial response of the glacier recession is an increase in sediment export, this is countered through the effects of sediment reworking through fluvial transport that reduces the downstream connectivity of sediment flux and makes it more dependent upon extreme sediment transport events. Similarly, whilst gully erosion into debuttressed Little Ice Age moraine is critical to connect upper sub-basins to the proglacial area, this process also produces very coarse material (material that could not be transported by the proglacial stream) that accumulates at the gully toes, serving to disconnect the system. Again, an initial response might be an increase in sediment transfer but as very coarse material accumulates, so it acts as a source of disconnection. Thus, there is a series of negative feedbacks in the system that serve to counter the effects of glacier recession on sediment yield.

In the next stage of analysis, work is needed in three areas. First, closer attention needs to be given to the evolution of grain size in space and in time, to quantify the possible impacts of sediment sorting upon sediment transfer and hence export. New surveillance technologies (e.g. drone technologies) should make this much easier than has hitherto been the case. Second, the analysis of connectivity could be taken further to consider all of the DEM data and at the full scale of the glacier system. It should also seek to quantify how temperature is changing the availability of sediment that can be mobilised through permafrost degradation higher in the basin and how readily such sediment sources are coupled to the channel network. Third, and most importantly, these kinds of analyses should be combined with graph theory methods (e.g.

Heckmann and Schwanghart, 2013) to quantify how sediment can flux through these landscapes and crucially, through using historically acquired data on glacier extent and the associated evolution of connectivity, how that sediment flux might have changed.

Conclusions

The analysis of a valuable record of hydroelectric power intake flushing, for a rapidly deglaciating Alpine drainage basin revealed systematic variability in sediment export between the late 1970s and present. Sediment export rates were high but variable until the early 1990s, then diminished before rising again from the early 2000s. An obvious explanation of this variability is a systematic variation in sediment transport capacity. Standardisation of the sediment export using a model of sediment transport capacity did not change this variability substantially, suggesting that the variability in export is not only a function of capacity limitation.

Initial considerations suggested that the effects of glacier recession on sediment connectivity could explain at least some of this process. An increase in connectivity following from reduction of the glaciated extent, expansion of the proglacial area, and the development of better connection between upper basins and the proglacial area, was to some extent identified in the data available. However, acceleration and deceleration of glacier recession appeared to lead to acceleration and deceleration of sediment export. It is hypothesised that river reworking of glacial till reduces sediment transfer through the proglacial zone. Coarse sediment accumulation at the base of gullies further serves to increase disconnection. These two negative feedbacks mean that continued exposure of unworked till is necessary to sediment transfer and export.

Finally, it was intriguing to find that since the early 2000s, sediment export from the basin has become dependent upon temperature. It was not possible to distinguish clearly whether this was because: (a) rising temperatures have led to permafrost degradation at higher altitudes, maintaining the supply of poorly consolidated sediment, and hence sediment transfer and export; or (b) whether it was now easier to identify temperature effects because the basin has become, in general, better connected. Field investigation of the state of permafrost in the upper part of the basin is required to evaluate these two hypotheses.

Acknowledgements

Grande Dixence SA, Alpiq SA and Hydroexploitation SA gave permission to use the discharge data and arranged for their supply to us and the assistance of Christian Constantin, Damien Courtine, Michel Follonier and Mike Imboden, of Hydroexploitation, is particularly appreciated. SwissTopo provided the unprocessed, scanned imagery. The project was supported by the Fonds Nationales Suisse SEDFATE project, awarded to Fritz Schlunegger, Stuart Lane, Jean-Luc Loizeau and Peter Molnar. The paper benefitted from critical but constructive comments from Sarah Rathburn, Ellen Wohl and two anonymous reviewers.

References

Arnold, N.S., 2010. A new approach for dealing with depressions in digital elevation models when calculating flow accumulation values. *Progress in Physical Geography*, 34, 781-809

Ashworth, P.J., Ferguson, R.I., Ashmore, P.E., Paola, C., Powell, D.M. and Prestegaard, K.L., 1992. Measurements in a braided river chute and lobe. 2. Sorting of bedload during entrainment, transport and deposition. *Water Resources Research*, 28, 1887-96

Bacchi, V., Recking, A., Eckert, N., Frey, P., Piton, G. and Naaim, M., 2014. The effects of kinetic sorting on sediment mobility on steep slopes. *Earth Surface Processes and Landforms*, 39, 1075-86

Baewert, H. and Morche, D., 2014. Coarse sediment dynamics in a proglacial fluvial system (Fagge River, Tyrol). *Geomorphology*, 218, 88-97

Ballantyne, C.K., 2002. Paraglacial geomorphology. *Quaternary Science Reviews*, 21, 1935–2017

Ballantyne, C.K., 2003. Paraglacial landform succession and sediment storage in deglaciated mountain valleys: theory and approaches to calibration. *Zeitschrift für Geomorphologie*. 32, 1–18

Banwell, A.F., Willis, I.C. and Arnold, N.S., 2013. Modeling subglacial water routing at Paakitsoq, W Greenland. *Journal of Geophysical Research: Earth Surface*, 118, doi:10.1002/jgrf.20093

Barry, R.G., 2006. The status of research on glaciers and global glacier recession: a review. *Progress in Physical Geography*, 30, 285–306

Bennett, G.L., Molnar, P., McArdell, B.W. and Burlando, P., 2014. A probabilistic sediment cascade model of sediment transfer in the Illgraben. *Water Resources Research*, 50, 1225-44

Bennett, G.L., Molnar, P., McArdell, B.W., Schlunegger, F. and Burlando, P., 2013. Patterns and controls of sediment production, transfer and yield in the Illgraben. *Geomorphology*, 188, 68-82

Bezinge, A., Clark, M.J., Gurnell, A.M. and Warburton, J., 1989. The management of sediment transported by glacial melt-water streams and its significance for the estimation of sediment yield. *Annals of Glaciology*, 13, 1-5

Bogen, J., 1989. Glacial sediment production and development of hydro-electric power in glacierized areas. *Annals of Glaciology*, 13, 6–11

Bogen, J., Xu, M,. and Kennie, P., 2015. The impact of pro-glacial lakes on downstream sediment delivery in Norway. *Earth Surface Processes and Landforms,* 40, 942–952.

Bosson, J., Deline, P., Bodin, X., Schoeneich, P., Baron, L., Gardent, M. and Lambiel, C., 2015 The influence of ground ice distribution on geomorphic dynamics since the Little Ice Age in proglacial areas of two cirque glacier systems. *Earth Surface Processes and Landforms*, 40, 666–680

Brock, B.W., Willis, I.C. and Sharp, M.J., 2000. Measurement and parameterization of albedo variations at Haut Glacier d'Arolla, Switzerland. *Journal of Glaciology*, 46, 675-688.

Brock, B.W., Willis, I.C. and Sharp, M.J., 2006. Measurement and parameterization of aerodynamic roughness length variations at Haut Glacier d'Arolla, Switzerland. *Journal of Glaciology*, 52, 281-297

Caine, N. and Swanson, S.F., 1989. Geomorphic coupling of hillslope and channel systems in two small mountain basins. *Zeitschrift für Geomorphologie*, 33, 189–203

Caine, N., 1976. A uniform measure of subaerial erosion. *Geological Society of America Bulletin*, 87, 137–140

Carling, P.A. and Reader, N.A., 1982. Structure, composition and bulk properties of upland stream gravels. *Earth Surface Processes and Landforms*, 7, 349–365

Carrivick, J.L. and Tweed, F.S., 2013. Proglacial lakes: character, behaviour and geological importance. *Quaternary Science Reviews*, 78, 34-52

Carrivick, J.L., 2007. Hydrodynamics and geomorphic work of jökulhlaups (glacial outburst floods) from Kverkfjöll volcano, Iceland. *Hydrological Processes*, 21, 725–740

Carrivick, J.L., Russell, A.J., and Tweed, F.S., 2004. Geomorphological evidence for jo˙kulhlaups from Kverkfjoöll volcano, Iceland. *Geomorphology*, 63, 81–102

Cavalli, M., Trevisani, S., Comiti, F. and Marchi, L., 2013. Geomorphometric assessment of spatial sediment connectivity in small Alpine catchments. *Geomorphology,* 188, 31-41

Chiarle, M., Iannotti, S., Mortara, G. and Deline, P., 2007. Recent debris flow occurrences associated with glaciers in the Alps. *Global and Planetary Change*, 56, 123-36

Church, M.A. and Ryder, J.M., 1972. Paraglacial sedimentation: a consideration of fluvial processes conditioned by glaciation. *Geological Association of America Bulletin,* 83, 3059–3071

Cossart, E. and Fort, M., 2008. Sediment release and storage in early degla- ciated areas: towards an application of the exhaustion model from case of massif des Ecrins (French Alps) since the Little Ice Age. *Norsk Geografisk Tidsskrift – Norwegian Journal of Geography*, 62, 115–131

Cossart, E., 2008. Landform connectivity and waves of negative feedbacks during the paraglacial period, a case study: the Tabuc subcatchment since the end of the Little Ice Age (massif des Ecrins, France). *Géomorphologie*: *Relief, Processus, Environnement*, 4, 249-60

Curry, A.M., Cleasby, V. and Zukowskyj, P., 2006. Paraglacial response of steep, sediment-mantled slopes to post-"Little Ice Age' glacier recession in the central Swiss Alps. *Journal of Quaternary Science*, 21, 211-25

Dadic, R., Mott, R., Lehning, M. and Burlando, P., 2010. Wind influence on snow depth distribution and accumulation over glaciers. *Journal of Geophysical Research*: *Earth Surface*, 115(F01012), 1-8

Evatt, G.W., Fowler, A.C., Clark, C.D., and Hulton, N.R.J., 2006. Subglacial floods beneath ice sheets. *Philosophical Transactions of the Royal Society*, A, 374, 1769–1794

Ferguson, R.I. 2007. Flow resistance equations for gravel- and boulder-bed streams. *Water Resources Research*, 43, W05427

Fischer, U., Mair, D., Kavanaugh, J., Willis, I., Nienow, P. and Hubbard, B., 2011. Modelling ice-bed coupling during a glacier speed-up event: Haut Glacier d'Arolla, Switzerland. *Hydrological Processes*, 25, 1361-1372

Fischer, M., Huss, M., and Hoelzle, M , 2015. Surface elevation and mass changes of all Swiss glaciers 1980-2010. *Cryosphere*, 9, 525-40

Fischer, M., Huss, M., Barboux, C. and Hoelzle, M., 2014. The new Swiss Glacier Inventory SGI2010: Relevance of using high-resolution source data on areas dominated by very small glaciers. *Arctic, Antarctic, and Alpine Research*, 46, 933-45

Gabbud, C., Micheletti, N. and Lane, S.N., 2016. Response of a temperate Alpine valley glacier to climate change at the decadal scale. Paper forthcoming in *Geografiska Annaler A – Physical Geography*

Gabbud, C. Micheletti, N. and Lane, S.N., 2015. LIDAR measurement of surface melt for a temperate Alpine glacier at the seasonal and hourly scales. *Journal of Glaciology*, 61, 963-74

Geilhausen, M., Morche, D., Otto, J.C., and Schrott, L., 2013. Sediment discharge from the proglacial zone of a retreating alpine glacier. *Zeitschrift fur Geomorphologie*, 57, Supplementary Isssue 3, 29-53

Hallet, B., Hunter, L. and Bogen, J., 1996. Rates of erosion and sediment evacuation by glaciers: A review of field data and their implications. *Global and Planetary Change*, 12, 213-35

Harbor, J., Sharp, M., Copland, L., Hubbard, B., Nienow, P. and Mair, D., 1997. Influence of subglacial drainage conditions on the velocity distribution within a glacier cross section. *Geology*, 25, 739-742

Harbor, J. and Warburton, J., 1993. Relative rates of glacial and nonglacial erosion in alpine environments. *Arctic and Alpine Reearch*, 25, 1–7

Heckmann, T. and Schwanghart, W., 2013. Geomorphic coupling and sediment connectivity in an alpine catchment - Exploring sediment cascades using graph theory. *Geomorphology*, 182, 89-103

Heckmann, T., McColl, S. and Morche, D., in press. Retreating ice: research in proglacial areas matters. Forthcoming in *Earth Surface Processes and Landforms*

Hicks, D.M., McSaveney, M.J. and Chinn, T.J.H., 1990. Sedimentation in proglacial Ivory lake, Southern Alps, New Zealand. *Arctic and Alpine Research*, 22, 26- 42

Holmgren, P., 1994, Multiple flow direction algorithms for runoff modelling in grid based elevation models: An empirical evaluation. *Hydrological Processes*, 8, 327–334

Hooke, J.M., 2003. Coarse sediment connectivity in river channel systems: a conceptual framework and methodology. *Geomorphology*, 56, 79-94

Hubbard, B. and Nienow, P., 1997. Alpine subglacial hydrology. Quaternary Science Reviews, 16, 939-955

Huggel, C., Clague, J.J. and Korup, O., 2012. Is climate change responsible for changing landslide activity in high mountains? *Earth Surface Processes and Landforms*, 37, 77–91

Hunter, L.E., Powell, R.D. and Lawson, D.E., 1996. Flux of debris transported by ice at three Alaskan tidewater glaciers. *Journal of Glaciology*, 42, 123–135

Kneisel, C., Rothenbühler, C., Keller, F. and Haeberli, W., 2007. Hazard assessment of potential periglacial debris flows based on GIS-based spatial modelling and geophysical field surveys: a case study in the Swiss Alps. *Permafrost and Periglacial Processes*, 18, 259–268

Kociuba, W. and Janicki, G., 2014. Continuous measurements of bedload transport rates in a small glacial river catchment in the summer season (Spitsbergen). *Geomorphology*, 212, 58-71

Kociuba, W. and Janicki, G., 2015. Changeability of Movable Bed-Surface Particles in Natural, Gravel-Bed Channels and Its Relation to Bedload Grain Size Distribution (Scott River, Svalbard). *Geografiska Annaler*, 97A, 507-21

Koppes, M.N. and Montgomery, D.R, 2009. The relative efficacy of fluvial and glacial erosion over modern to orogenic timescales. *Nature Geoscience*, 2, 644-647

Lamoureux, S.F., 2002. Temporal patterns of suspended sediment yield following moderate to extreme hydrological events recorded in varved lacustrine sediments. *Earth Surface Processes and Landforms*, 27, 1107–1124

Lane, S.N., Widdison, P.E., Thomas, R.E., Ashworth, P.J., Best, J.L., Lunt, I.A., Sambrook Smith, G.H. and Simpson, C.L., 2010. Quantification of braided river channel change using archival digital image analysis. *Earth Surface Processes and Landforms*, 35, 971-85

Lane, S.N., Richards, K.S. and Chandler, J.H., 1996. Discharge and sediment supply controls on erosion and deposition in a dynamic alluvial channel. *Geomorphology*, 15, 1-15

Lane, S.N., Reid, S.C., Westaway, R.M. and Hicks, D.M., 2004. Remotely sensed topographic data for river channel research: the identification, explanation and management of error. In Kelly, R.E.J., Drake, N.A. and Barr, S.L., Spatial Modelling of the Terrestrial Environment, Wiley, Chichester, 157-74

Lane, S.N., Richards, K.S. and Chandler, J.H. 1995. Morphological estimation of the time-integrated bedload transport rate. *Water Resources Research*, 31, 761-72

Lane, S.N., 1997. The reconstruction of bed material yield and supply histories in gravel-bed streams. *Catena*, 30, 183-96

Leggat, M.S., Owens, P.N., Stott, T.A., Forrester, B.J., Déry, S.J. and Menounos, B., 2015. Hydro-meteorological drivers and sources of suspended sediment flux in the pro-glacial zone of the retreating Castle Creek Glacier, Cariboo Mountains, British Columbia, Canada. *Earth Surface Processes and Landforms*, 40, 1542-1559

Lugon R. and Stoffel, M., 2010. Rock–glacier dynamics and magnitude–frequency relations of debris flows in a high-elevation watershed: Ritigraben, Swiss Alps. *Global and Planetary Change*, 73, 202–210

Mair, D., Willis, I., Fischer, U., Hubbard, B., Nienow, P. and Hubbard, A., 2003. Hydrological controls on patterns of surface, internal and basal motion during three “spring events”: Haut Glacier d’Arolla, Switzerland. *Journal of Glaciology*, 49, 555-567

Mair, D., Nienow, P., Sharp, M., Wohlleben, T. and Willis, I., 2002. Influence of subglacial drainage system evolution on glacier surface motion: Haut Glacier d’Arolla, Switzerland. *Journal of Geophysical Research: Earth Surface*, 107, X-1 - X-13

Marren, P.M. and Toomath, S.C., 2014. Channel pattern of proglacial rivers: topographic forcing due to glacier retreat. *Earth Surface Processes and Landforms*, 39, 943–951

Mercier, D., 2008. Paraglacial and paraperiglacial landsystems: concepts, temporal scales and spatial distribution. *Géomorphologie*: *Relief, Processus, Environnement*, 4, 223–34

Mercier, D., Étienne, S., Sellier, D. and André, M.-F., 2009. Paraglacial gullying of sediment-mantled slopes: a case study of Colletthøgda, Kongsfjorden area, West Spitsbergen (Svalbard). *Earth Surface Processes and Landforms*, 34, 1772–1789

Messenzehl, K., Hoffmann, T. and Dikau, R., 2014. Sediment connectivity in the high-alpine valley of Val Muschauns, Swiss National Park - linking geomorphic field mapping with geomorphometric modelling. *Geomorphology*, 221, 215-29

Meyer-Peter, E., and Müller, R. 1948. Formulas for bed-load transport. Proc. 2nd IAHR Meeting, IAHR, Stockholm, 39-64

Micheletti, N., Lane, S.N. and Chandler, J.H., 2015a. Application of archival aerial photogrammetry to quantify climate forcing of Alpine landscapes. *Photogrammetric Record*, 30, 143-65

Micheletti, N., Lane, S.N. and Lambiel, C., 2015b. Investigating decadal scale geomorphic dynamics in an Alpine mountain setting. *Journal of Geophysical Research - Earth Surface*, 120, 2155-75

Morche, D., Haas, F., Baewert, H., Heckmann, T., Schmidt, K.-H. and Becht, M., 2012. Sediment transport in the proglacial Fagge River (Kaunertal/Austria). In Collins, A.L. *et al.* (Editors) *Erosion and Sediment Yields in the Changing Environment ,* IAHS Special Publication, 356, Wallingford, U.K., 72-80

Morche, D., Schmidt, K.H., Sahling, I., Herkommer, M. and Kutschera, J., 2008. Volume changes of Alpine sediment stores in a state of post-event disequilibrium and the implications for downstream hydrology and bed load transport. *Norsk Geografisk Tidsskrift - Norwegian Journal of Geography*, 62, 89-101

Nicholas, A.P. and Sambrook-Smith, G.S., 1998. Relationships between flow hydraulics, sediment supply, bedload transport and channel stability in the proglacial Virkisa River, Iceland. *Geografiska Annaler Series A, Physical Geography*, 80, 111-22

Nienow, P., Sharp, M. and Willis, I., 1998. Seasonal changes in the morphology of the subglacial drainage system, Haut Glacier d'Arolla, Switzerland. *Earth Surface Processes and Landforms*, 23, 825-843

Nienow, P.W., Hubbard, A.L., Hubbard, B.L., Chandler, D.M., Mair, D.W.F., Sharp, M.J. and Willis, I.C., 2005. Hydrological controls on diurnal ice flow variability in valley glaciers. *Journal of Geophysical Research: Earth Surface*, 110, 1-11

Nitsche, M., Rickenmann, D., Turowski, J.M., Badoux, A. and Kirchner, J.W. 2011. Evaluation of bedload transport predictions using flow resistance equations to account for macro-roughness in steep mountain streams. *Water Resources Research*, 47, WR010645.

Orwin, J., Lamoureux, S.F., Warburton, J. and Beylich, A., 2010. A framework for characterizing fluvial sediment fluxes from source to sink in cold environments. *Geografisker Annaler*, 92A, 155–176

Orwin, J.F. and Smart, C.C., 2004a: Short-term spatial and temporal patterns of suspended sediment transfer in proglacial channels, Small River Glacier, Canada. *Hydrological Processes*,18, 1521–1542

Orwin, J.F. and Smart, C.C., 2004b. The evidence for paraglacial sedimentation and its temporal scale in the deglacierizing basin of Small River Glacier, Canada. *Geomorphology*, 58, 175–202

Østrem, G., 1975. Sediment transport in glacial meltwater streams. In Jopling, A.V. and MacDonald, B.C. (Editors) *Glaciofluvial and glaciolacustrine sedimentation*, Society of Economic Paleontologists and Mineralogists, 23, 101-22

Otto, J.C., Schrott, L., Jaboyedoff, M. and Dikau, R., 2009. Quantifying sediment storage in a high alpine valley (Turtmanntal, Switzerland). *Earth Surface Processes and Landforms*, 34, 1726-1742

Pellicciotti, F., Brock, B., Strasser, U., Burlando, P., Funk, M. and Corripio, J., 2005. An enhanced temperature-index glacier melt model including the shortwave radiation balance: development and testing for Haut Glacier d'Arolla, Switzerland. *Journal of Glaciology*, 57, 573-587

Peñuela, A., Javaux, M. and Bielders, C.L., 2015. How do slope and surface roughness affect plot-scale overland flow connectivity? *Journal of Hydrology*, 528, 192–205

Porter, P.R., Vatne, G., Ng, F. and Irvine-Fynn, T.D.L., 2010. Ice-marginal sediment delivery to the surface of a high-Arctic glacier: Austre Brøggerbreen, Svalbard. *Geografiska Annaler*, 92A, 437-449

Raymond Pralong, M., Turowski, J. M., Rickenmann, D., and Zappa, M., 2015. Climate change impacts on bedload transport in alpine drainage basins with hydropower exploitation. *Earth Surface Processes and Landforms*, 40, 1587–1599

Rickenmann, D., 1991. Hyperconcentrated flow and sediment transport at steep flow. *Journal of Hydraulic Engineering*, 117, 1419–1439

Rickenmann, D and Recking, A., 2011. Evaluation of flow resistance equations using a large field data base. *Water Resources Research*, 47, W07538

Rippin, D., Willis, I., Arnold, N., Hodson, A., Moore, J., Kohler, J. and Björnsson, H., 2003. Changes in geometry and subglacial drainage of Midre Lovénbreen, Svalbard, determined from digital elevation models. *Earth Surface Processes and Landforms*, 28 , 273–298

Santos-Gonzalez, J., Santos, J.A., Gonzalez-Gutierrez, R.B., Redondo-Vega, J.M. and Gomez-Villar, A., 2013. Till fabric and grain-size analysis of glacial sequences in the Upper Sil River Basin, Cantabrian Mountains, NW Spain. *Physical Geography*, 34, 471-90

Schiefer, E. and Gilbert, R., 2007. Reconstructing morphometric change in a proglacial landscape using historical aerial photography and automated DEM generation. *Geomorphology*, 88, 167-78

Schiefer, E. and Gilbert, R., 2008. Proglacial sediment trapping in recently formed Silt Lake, Upper Lillooet Valley, Coast Mountains, British Columbia. *Earth Surface Processes and Landforms*, 33, 1542–1556

Schwanghart, W. and Kuhn, K.J., 2010. TopoToolbox: a set of Matlab functions for topographic analysis. *Environmental Modelling and Software*, 25, 770-81

Sharp, M., Richards, K., Willis, I., Arnold, N., Nienow, P., Lawson, W. and Tison, J.-L., 1993. Geometry, bed topography and drainage system structure of the haut glacier d'Arolla, Switzerland. *Earth Surface Processes and Landforms*, 18, 557–571

Shreve, R.L., 1972. Movement of water in glaciers. *Journal of Glaciology*, 11, 205– 214

Slaymaker, O., Souch, C., Menounos, B. and Filippelli, G., 2003. Advances in Holocene mountain geomorphology inspired by sediment budget methodology. *Geomorphology*, 55, 305-316

Soar, P.J. and Thorne, C.R., 2001. *Channel Restoration Design for Meandering Rivers*. US Army Corps of Engineers Report ERDC/CHL CR-01-1, Washington, 416pp plus appendices.

Staines, K.E.H., Carrivick, J.L., Tweed, F.S., Evans, A.J., Russell, A.J., Jóhannesson, T., and Roberts, M., 2015. A multi- dimensional analysis of pro-glacial landscape change at Sólheimajökull, southern Iceland. *Earth Surface Processes and Landforms*, 40, 809–822

Stoffel, M. and Huggel, C., 2012. Effects of climate change on mass movements in mountain environments. *Progress in Physical Geography*, 36, 421-39

Stott, T., 2002. Bedload transport and channel bed changes in the proglacial Skeldal River, northeast Greenland. *Arctic, Antarctic and Alpine Research*, 34, 334-44

Swift, D.A., Nienow, P.W., Spedding, N. and Hoey, T.B., 2002. Geomorphic implications of subglacial drainage system configuration: rates of basal sediment evacuation controlled by seasonal drainage system evolution. *Sedimentary Geology*, 149, 5-19

Swift, D.A., Nienow, P.W. and Hoey, T.B., 2005. Basal sediment evacuation by subglacial meltwater: suspended sediment transport from Haut Glacier d'Arolla, Switzerland. *Earth Surface Processes and Landforms*, 30, 867–883

Trevisani, S., Cavalli, M. and Marchi, L, 2012. Surface texture analysis of a high-resolution DTM: Interpreting an alpine basin. *Geomorphology*, 161, 26-39

Uhlmann, M., Korup, O., Huggel, C., Fischer, L., Kargel, J.S. and 2013. Supra-glacial deposition and sediment flux of catastrophic rock-slope failure debris, south-central Alaska. *Earth Surface Processes and Landforms*, 38, 675–682

Vaughan, D.G., Comiso, J.C., Allison, I., Carrasco, J., Kaser, G., Kwok, R., Mote, P., Murray, T., Paul, F., Ren, J., Rignot, E., Solomina, O., Steffen, K. and Zhang, T., 2013. Observations: Cryosphere. In *Climate Change 2013: The Physical Science Basis*. Contribution of Working Group I to the Fifth Assessment Report of the Intergovernmental Panel on Climate Change, Stocker, T.F., Qin, D., Plattner, G.K., Tignor, M., Allen, S.K., Boschung, J., Nauels, A., Xia, Y., Bex, V. and Midgley, P.M. (eds), Cambridge University Press, Cambridge, 317–382.

Warburton, J., 1990a. An alpine proglacial fluvial sediment budget. *Geografiska Annaler*, 72A, 261–272

Warburton, J., 1990b. Observations of bedload transport can channel bed changes in a proglacial mountain stream. *Arctic and Alpine Research*, 24, 195-203

Wilcock, P. and Crowe, J. 2003. Surface-based transport model for mixed-size Sediment. *Journal of Hydraulic Engineering*, 129, 120–128

Willis, I., Mair, D., Hubbard, B., Nienow, P., Fischer, U. and Hubbard, A., 2003. Seasonal variations in ice deformation and basal motion across the tongue of Haut Glacier d'Arolla, Switzerland. *Annals of Glaciology*, 36, 157-167

Wold, B. and ∅strem, G., 1979. Subglacial constructions and investigations at Bondhusbreen, Norway. *Journal of Glaciology*, 23, 363-79

Wright, A.P., Siegert, M.J., Le Brocq, A.M., and Gore, D.B., 2008. High sensitivity of subglacial hydrological pathways in Antarctica to small ice-sheet changes. *Geophysical Research Letters*, 45, L17504

List of figures

Figure 1. Location of the study area (1a), an oblique aerial view (1b) taken from within the red bounding box looking towards the blue bounding box in 1a, and based upon 2014 imagery showing. 1b shows key elements of the study, including the flow intake, a schematic of which is shown in 1c.

Figure 2. Example of discharge data from the Haut Glacier d'Arolla intake. This shows a raw discharge time-series, the interpolated discharge during a purge, and the estimated flow release.

Figure 3. Modelled annual volumetric transport capacity and basin water yield.

Figure 4. Modelled annual volumetric transport capacity and estimated sediment export volume per year. The derivation of the error bars for the export volume is explained in the text.

Figure 5. A plot of the supply-capacity ratio through time. Also superimposed is the increase in proglacial area associated with recession of the Haut Glacier d'Arolla, with respect to its position in 1967 (5a) and the mean annual air temperature (5b) for Bricola, a south-facing weather station at an altitude of 2'430 m and 7.8 km North-North East of the current glacier terminus.

Figure 6. Orthoimages of the Haut Glacier d'Arolla proglacial area for 1967 (6a), 1977 (6b), 1983 (6c), 1988 (6d), 1997 (6e), 2000 (6f), 2005 (6g) and 2009 (6h). Long dashes show the glacier margin. Short dashes show the true right boundary between river worked sediment and morainic material. The bounding box in Figure 6e shows gullies that developed significantly between 1988 and 1997.

Figure 7. Comparison of slope maps for the proglacial area for 1997 and 2009, marking a part of the proglacial zone that contained ice cored moraine in 1997 but which had melted out by 2009. By 2009, this had resulted in a much wider proglacial channel.

Figure 8. The areas and dates when different parts of the proglacial zones became fluvially-reworked (8a) and the associated volumes of change by period (8b). The legend shows the first date in which aerial imagery suggests the proglacial area became fluvially reworked.

Figure 9. The logarithm of upslope contributing area (shading) shown for 2009 for the east side of the basin. Also marked are the digitised eastern extent of the glacier in 1967 and in 2005 (white lines) and the locations (white boxes) used to quantify changes in connectivity between 1967 and 2009 in Figure 10. The colour bar shows the logarithm of the upslope contributing area (in m^2).

Figure 10. Plots of the upslope contributing area obtained for different levels of DEM fill (x axis) for different values of the flow routing parameter *x* (in [5]), shown in the legend. Plots are shown for four basins marked on Figure 9 as white boxes from left (sub basin 1) through to right (sub basin 4), and for the years 1967 and 2014.

Figure 11. DEMs of difference for four periods (11a through 11d) and associated slope maps at the end of each period (11e through 11h).

Figure 12. Across hillslope profile showing the evolution of the gully connecting sub basin 4 to the proglacial area from 1983 to 2009 (the left gully) plus the two adjacent gullies.

Figure 13. Cumulative probability plots of water yield and sediment transport capacity for the year 2014.

Figure 14. Summary of key processes controlling sediment flux to the basin outlet. We identify key processes that limit connectivity before glacier recession ("pre-recession"), the key changes that directly influence connectivity as a result of "glacier recession" and then what happens to the side walls and the proglacial area post-recession.

List of Tables

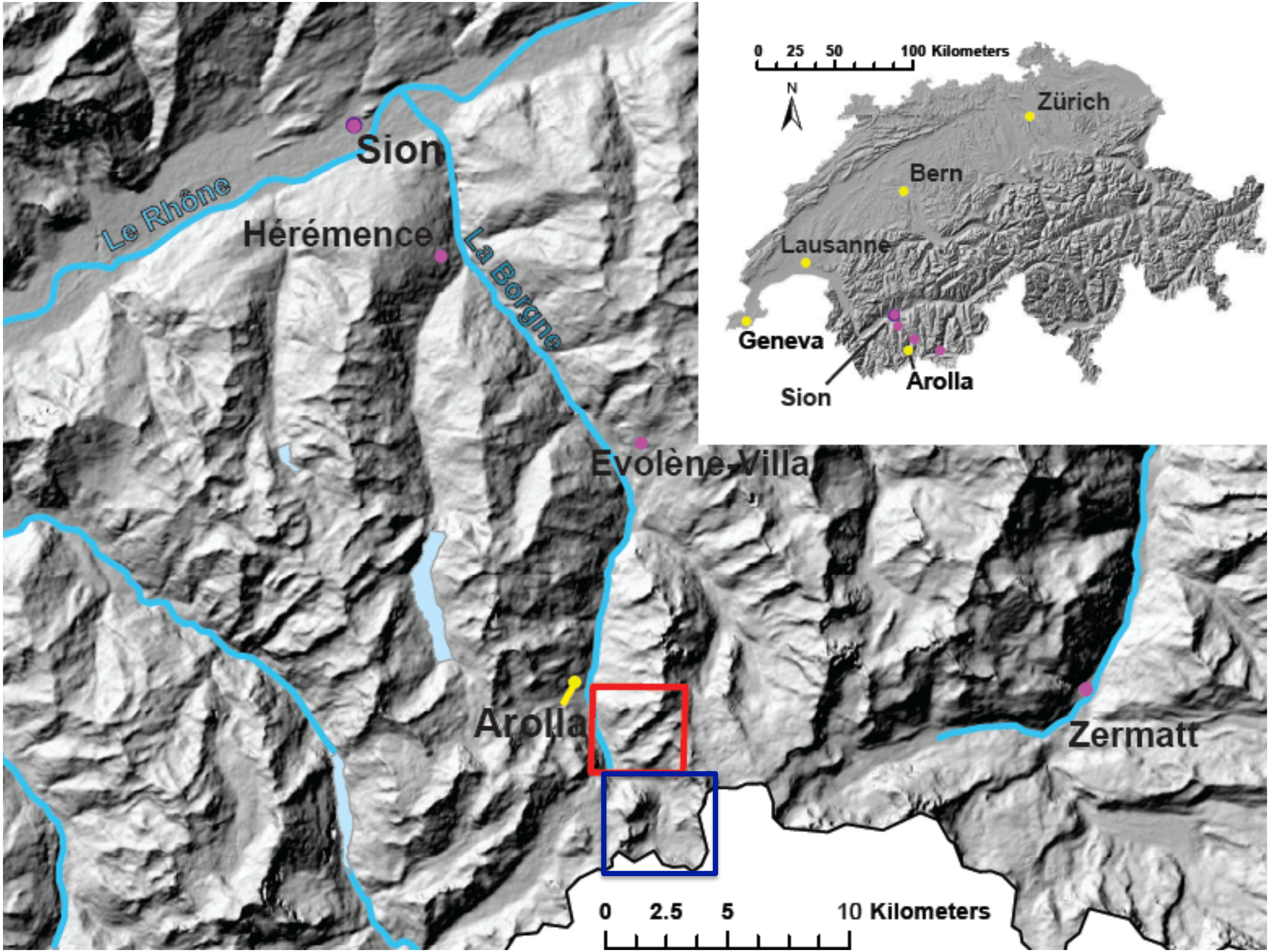

Sion
Le Rhône
Hérémence
La Borgne
Evolène-Villa
Arolla
Zermatt
0 2.5 5 10 Kilometers
0 25 50 100 Kilometers
N
Zürich
Bern
Lausanne
Geneva
Sion
Arolla

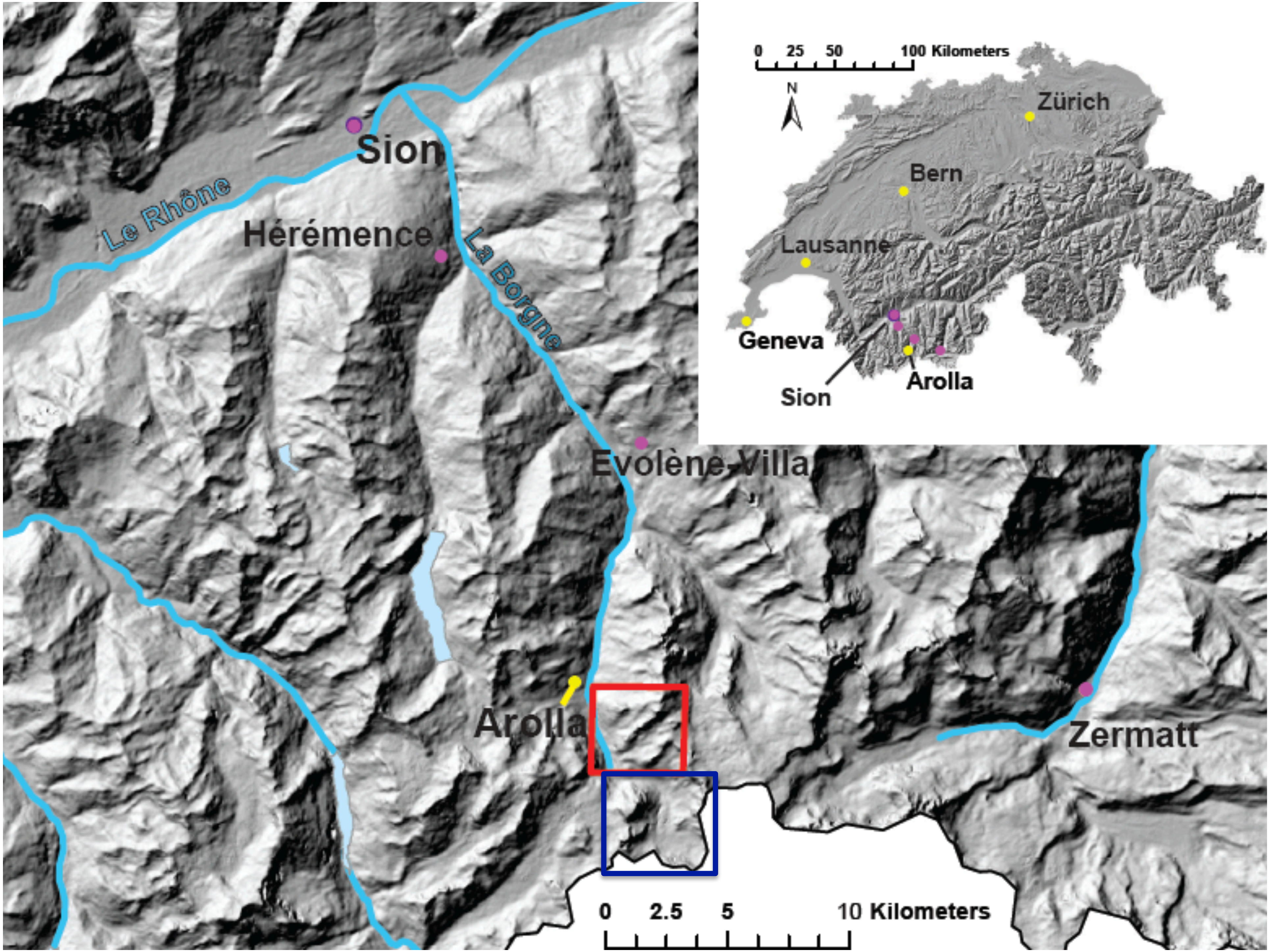

Sion
Le Rhône
Hérémence
La Borgne
Evolène-Villa
Arolla
Zermatt
0 2.5 5 10 Kilometers
0 25 50 100 Kilometers
N
Zürich
Bern
Lausanne
Geneva
Sion
Arolla

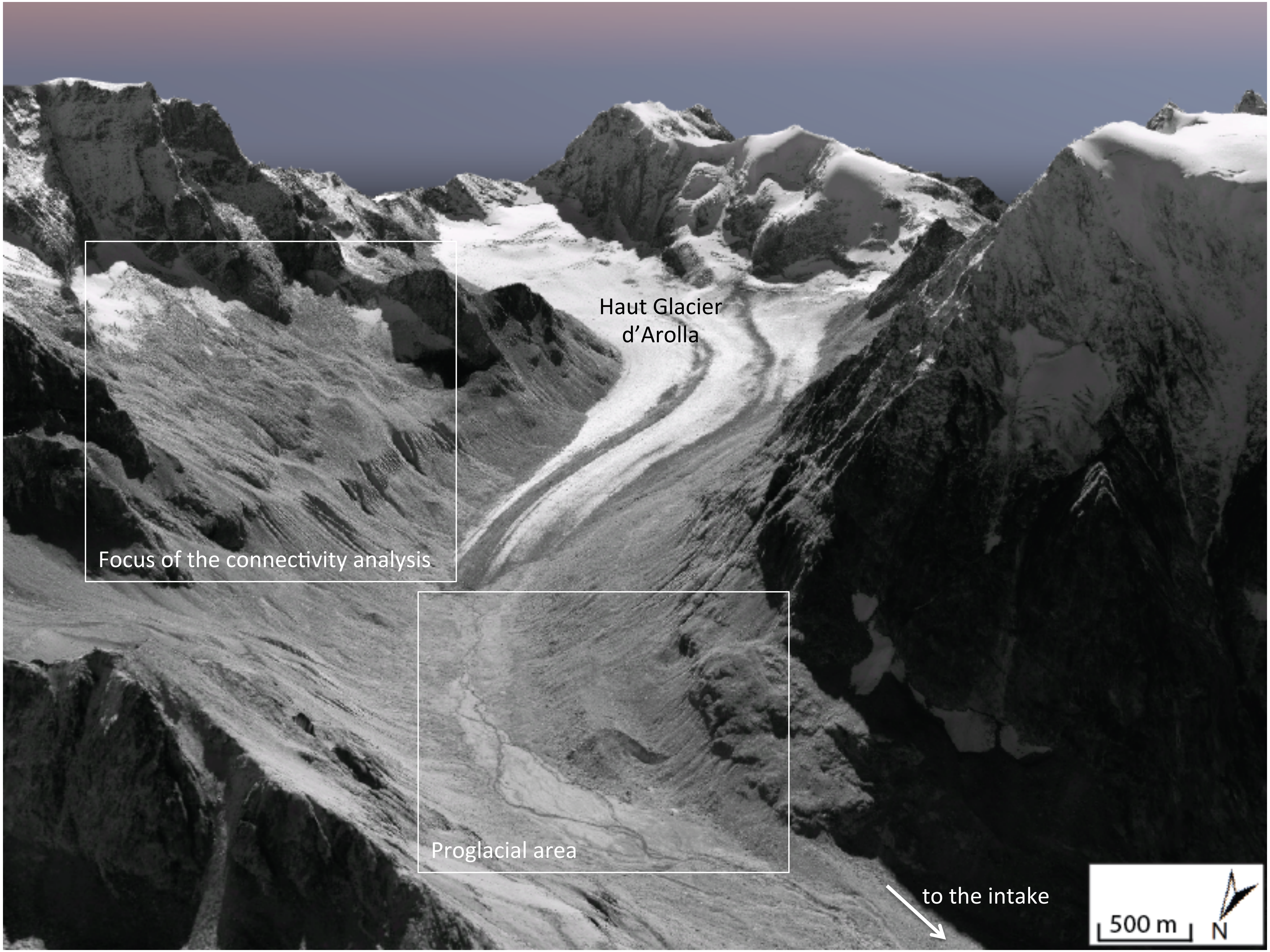
Haut Glacier
d'Arolla
Focus of the connectivity analysis
Proglacial area
to the intake
500 m
N

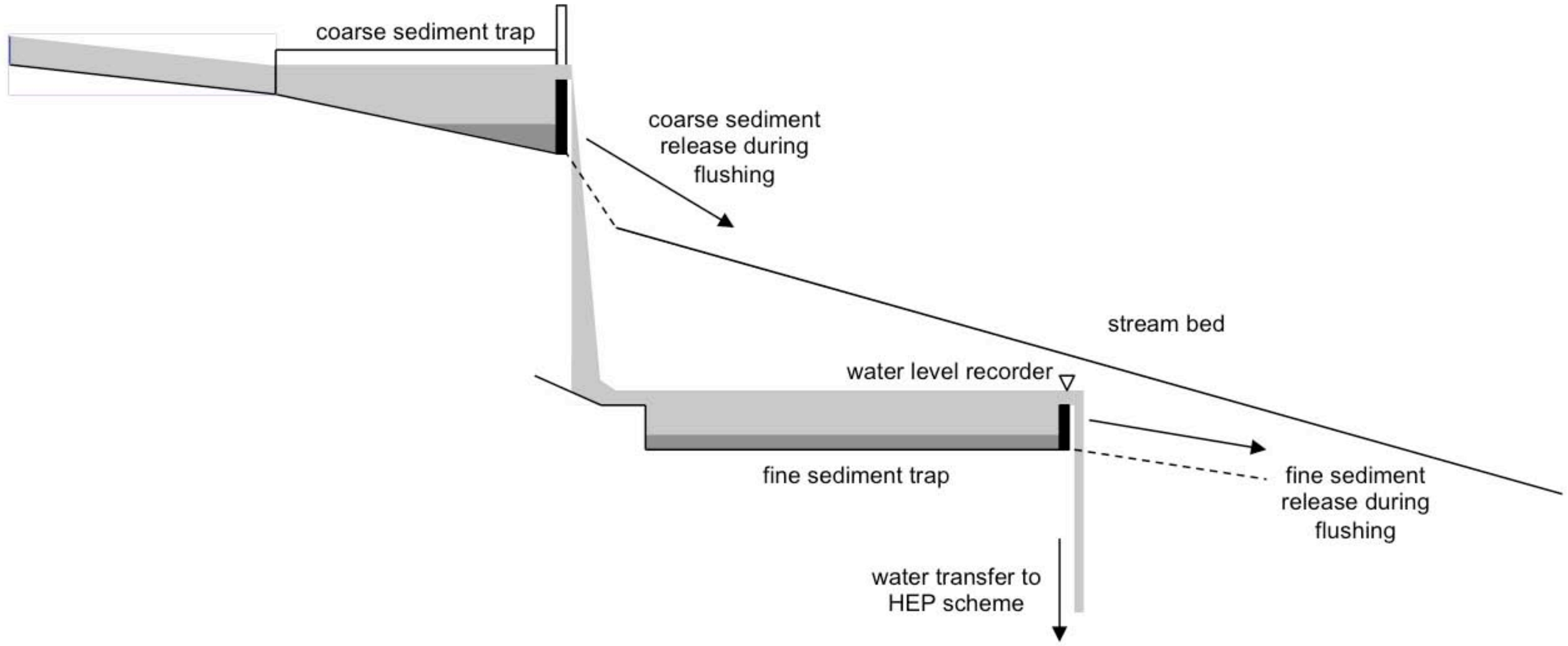
coarse sediment trap
coarse sediment
release during
flushing
stream bed
water level recorder
fine sediment trap
fine sediment
release during
flushing
water transfer to
HEP scheme

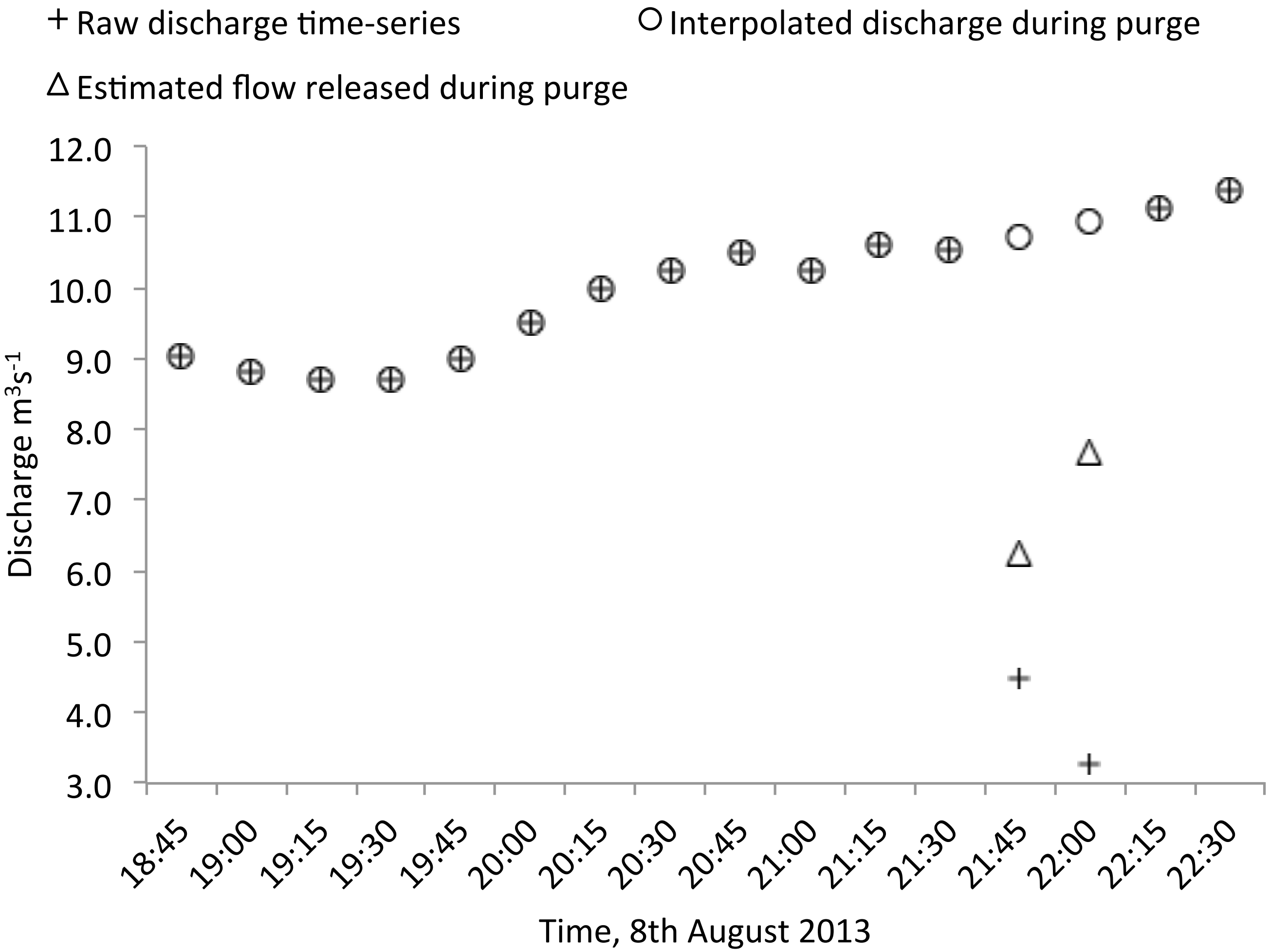
+ Raw discharge time-series
○ Interpolated discharge during purge
△ Estimated flow released during purge
12.0
11.0
10.0
9.0
8.0
7.0
6.0
5.0
4.0
3.0
Discharge m3s-1
18:45
19:00
19:15
19:30
19:45
20:00
20:15
20:30
20:45
21:00
21:15
21:30
21:45
22:00
22:15
22:30
Time, 8th August 2013

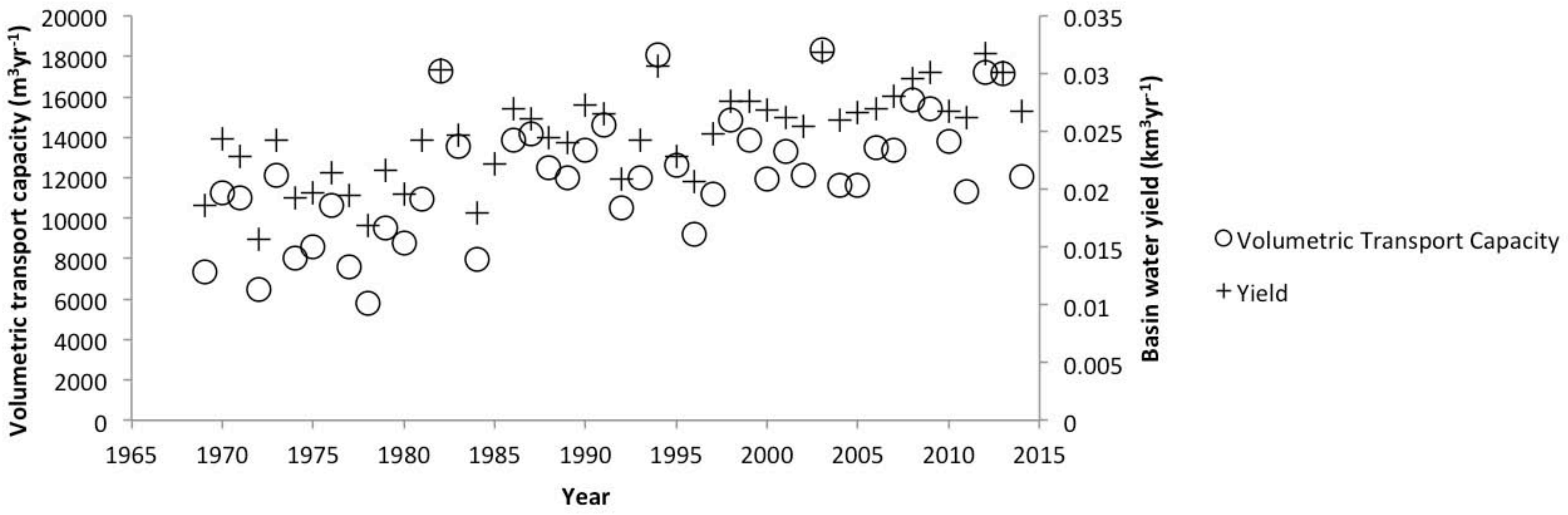

Volumetric transport capacity (m^3yr^{-1})
Basin water yield (km^3yr^{-1})
Year
Volumetric Transport Capacity
Yield
20000
18000
16000
14000
12000
10000
8000
6000
4000
2000
0
0.035
0.03
0.025
0.02
0.015
0.01
0.005
0
1965
1970
1975
1980
1985
1990
1995
2000
2005
2010
2015

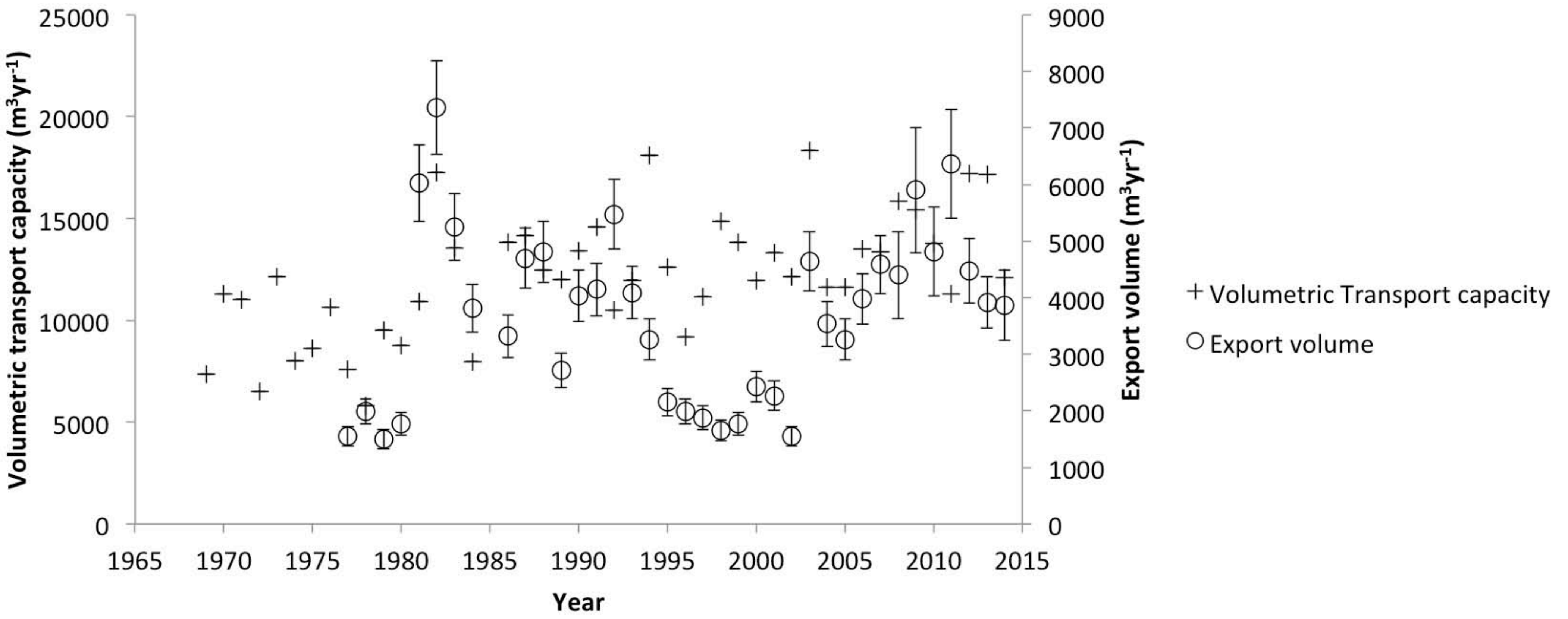

Volumetric transport capacity (m3yr-1)
Export volume (m3yr-1)
Year
+ Volumetric Transport capacity
Export volume
25000
20000
15000
10000
5000
0
9000
8000
7000
6000
5000
4000
3000
2000
1000
0
1965
1970
1975
1980
1985
1990
1995
2000
2005
2010
2015

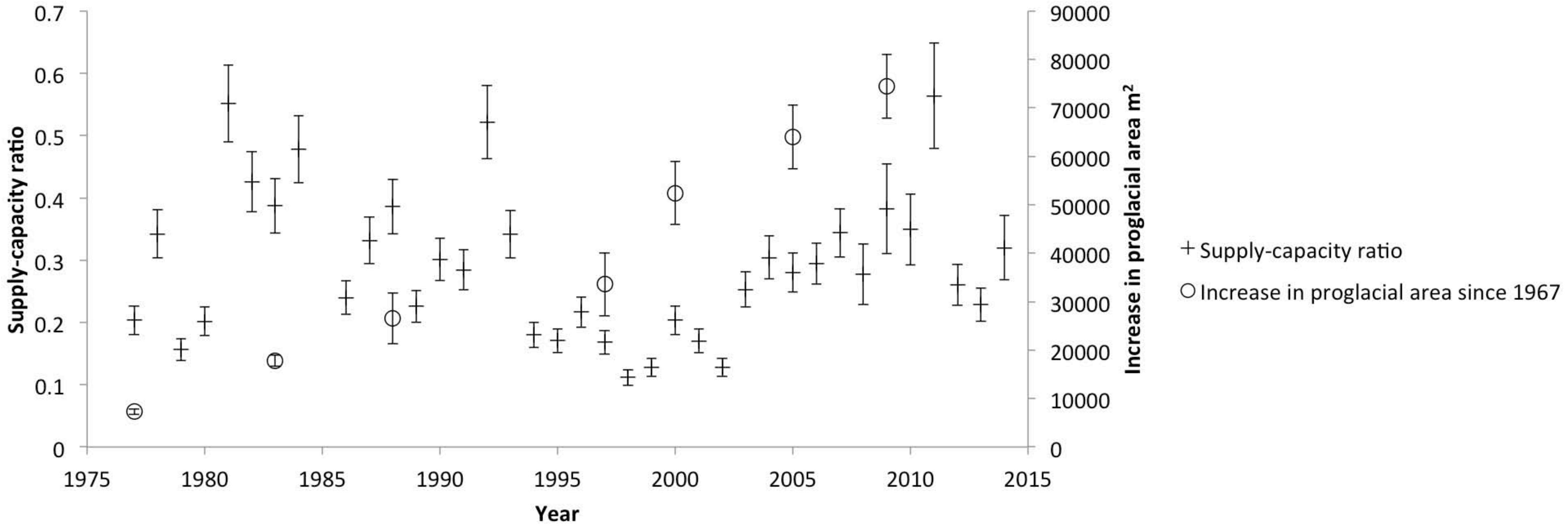

0.7
0.6
0.5
0.4
0.3
0.2
0.1
0
Supply-capacity ratio
90000
80000
70000
60000
50000
40000
30000
20000
10000
0
Increase in proglacial area m²
1975
1980
1985
1990
1995
2000
2005
2010
2015
Year
Supply-capacity ratio
Increase in proglacial area since 1967

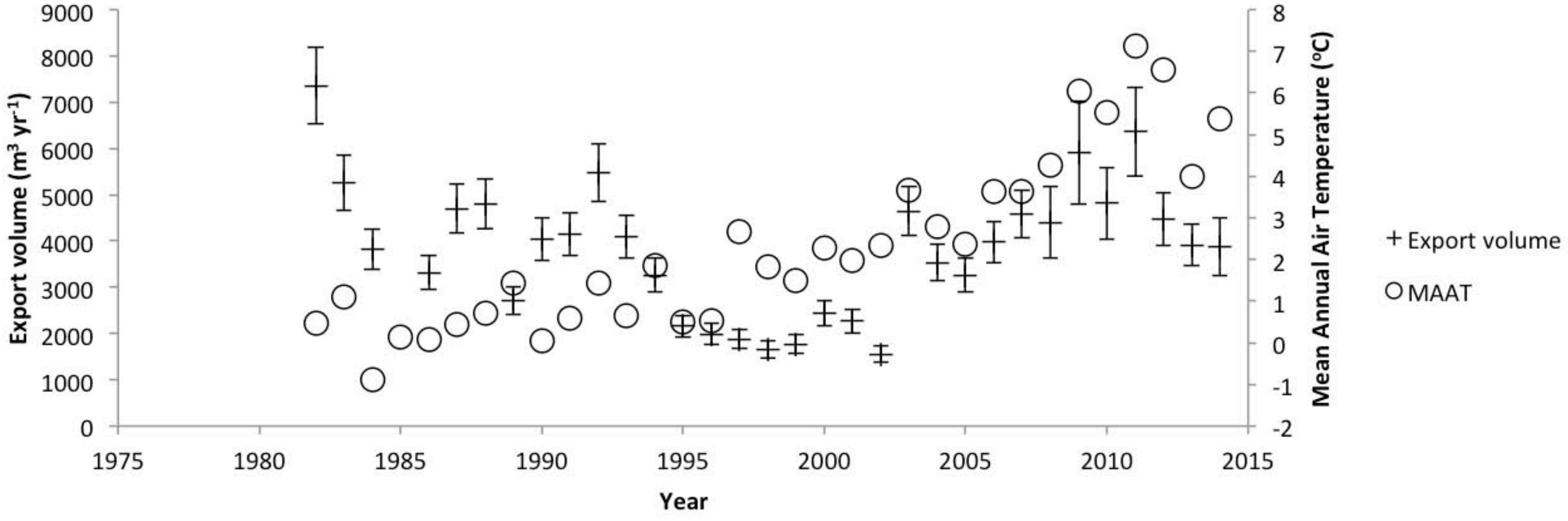
Export volume (m^3 yr^{-1})
Mean Annual Air Temperature (°C)
Year
9000
8000
7000
6000
5000
4000
3000
2000
1000
0
8
7
6
5
4
3
2
1
0
-1
-2
1975
1980
1985
1990
1995
2000
2005
2010
2015
+ Export volume
MAAT

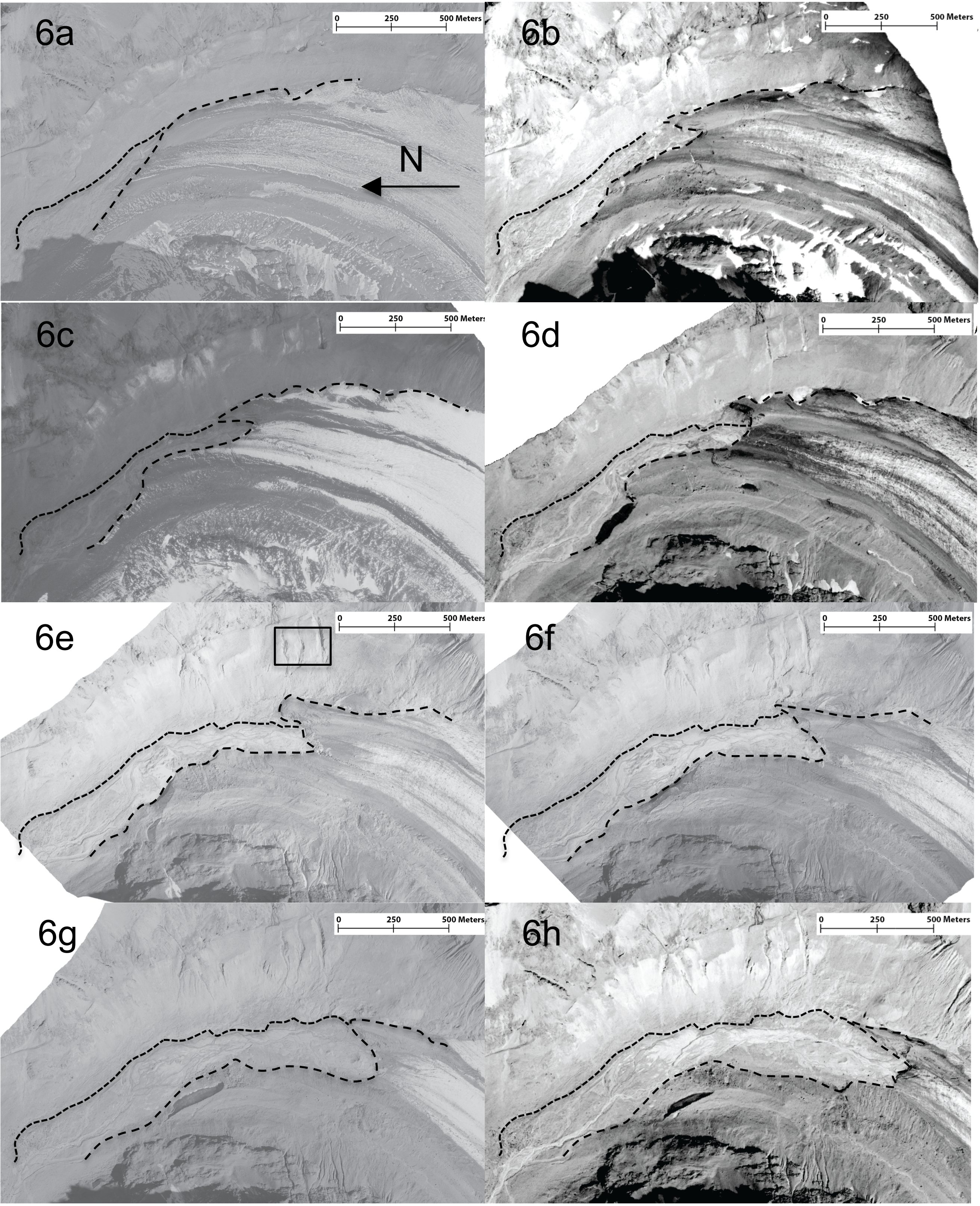
6a
0 250 500 Meters
N
6b
0 250 500 Meters
6c
0 250 500 Meters
6d
0 250 500 Meters
6e
0 250 500 Meters
6f
0 250 500 Meters
6g
0 250 500 Meters
6h
0 250 500 Meters

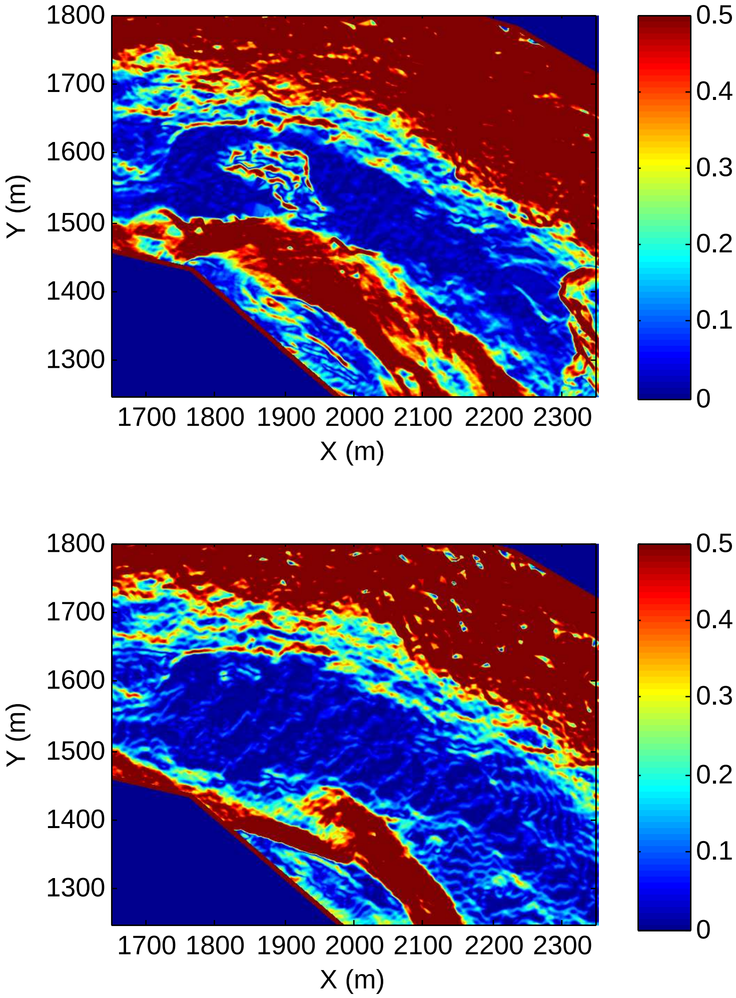
1800
1700
1600
1500
1400
1300
Y (m)
1700 1800 1900 2000 2100 2200 2300
X (m)
0.5
0.4
0.3
0.2
0.1
0
1800
1700
1600
1500
1400
1300
Y (m)
1700 1800 1900 2000 2100 2200 2300
X (m)
0.5
0.4
0.3
0.2
0.1
0

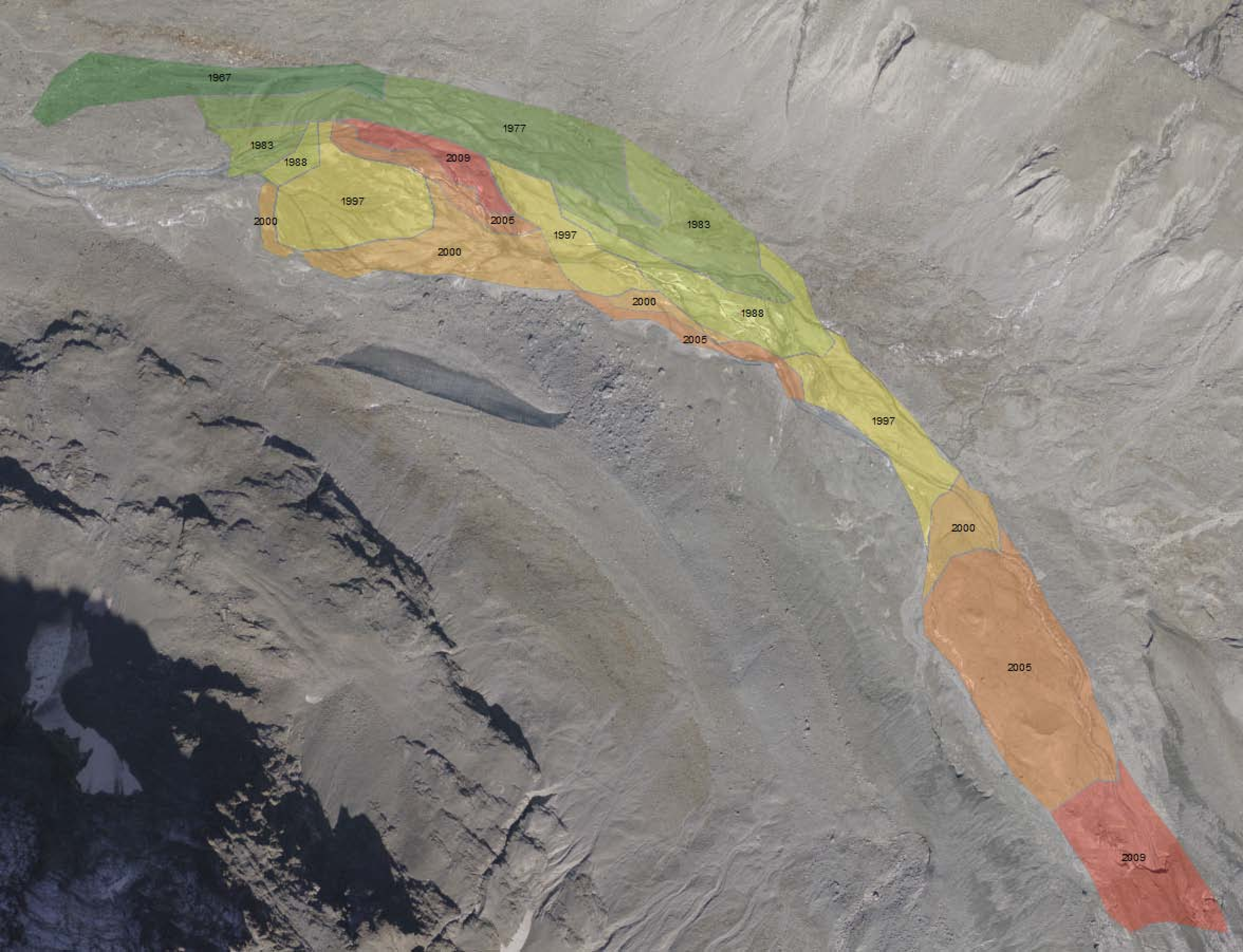
1967
1977
1983
1988
2009
1997
2000
2005
1997
1983
2000
2000
1988
2005
1997
2000
2005
2009

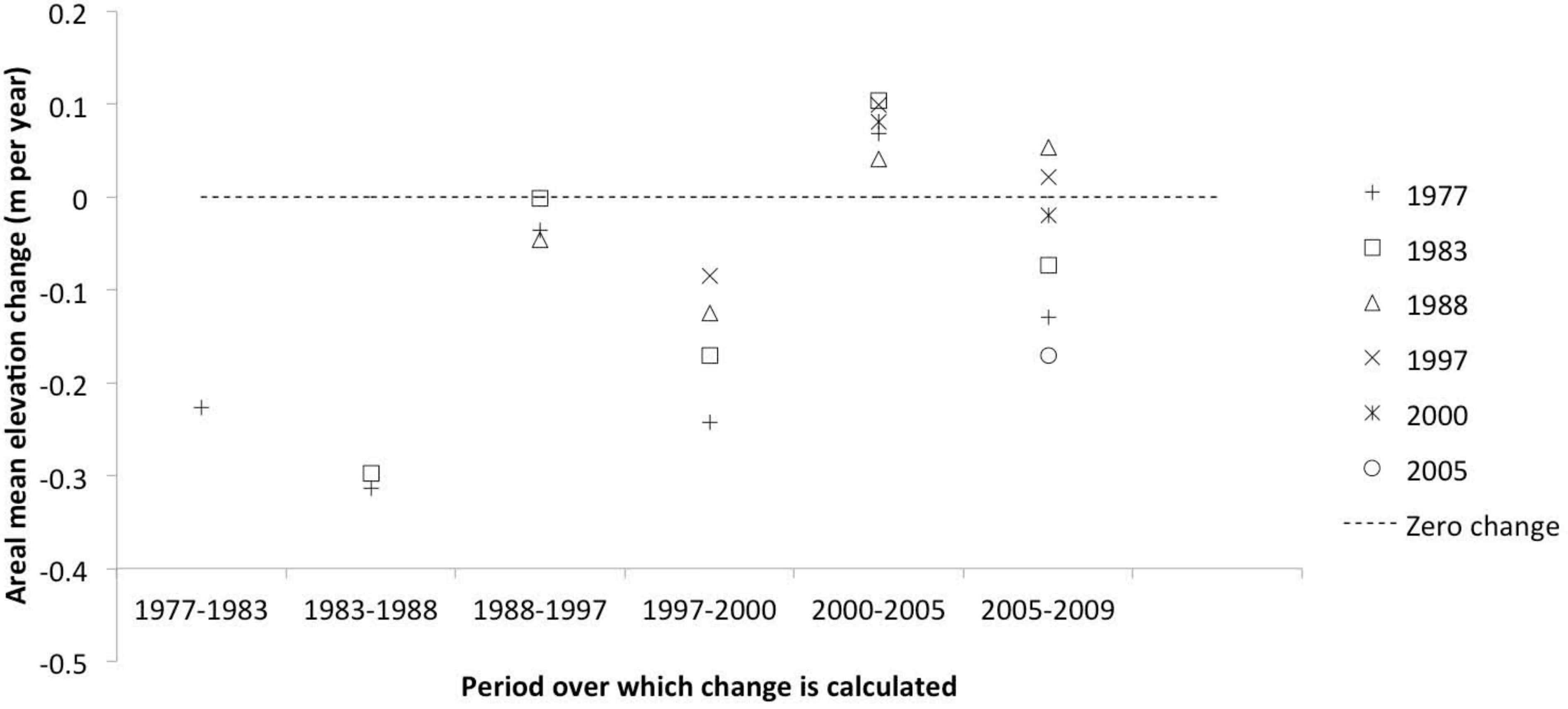
0.2
0.1
0
-0.1
-0.2
-0.3
-0.4
-0.5
Areal mean elevation change (m per year)
1977-1983
1983-1988
1988-1997
1997-2000
2000-2005
2005-2009
Period over which change is calculated
1977
1983
1988
1997
2000
2005
Zero change

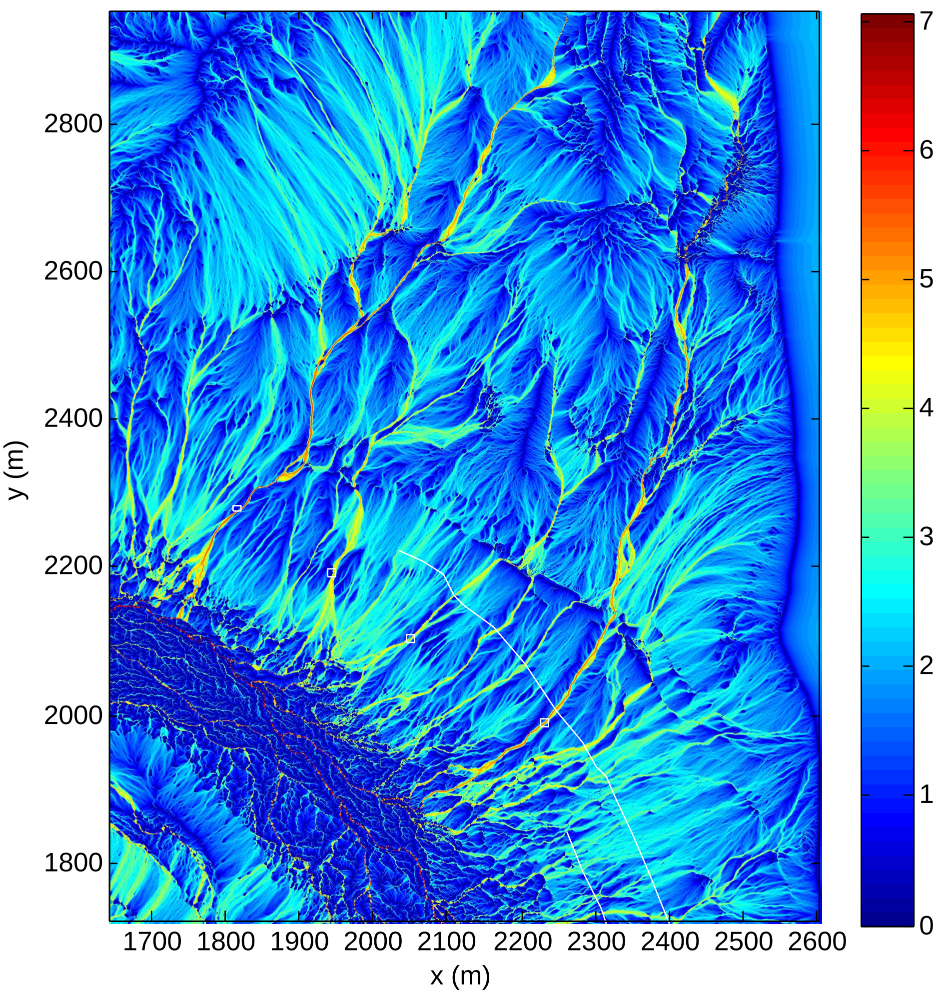

2800
2600
2400
2200
2000
1800
y (m)
1700 1800 1900 2000 2100 2200 2300 2400 2500 2600
x (m)
7
6
5
4
3
2
1
0

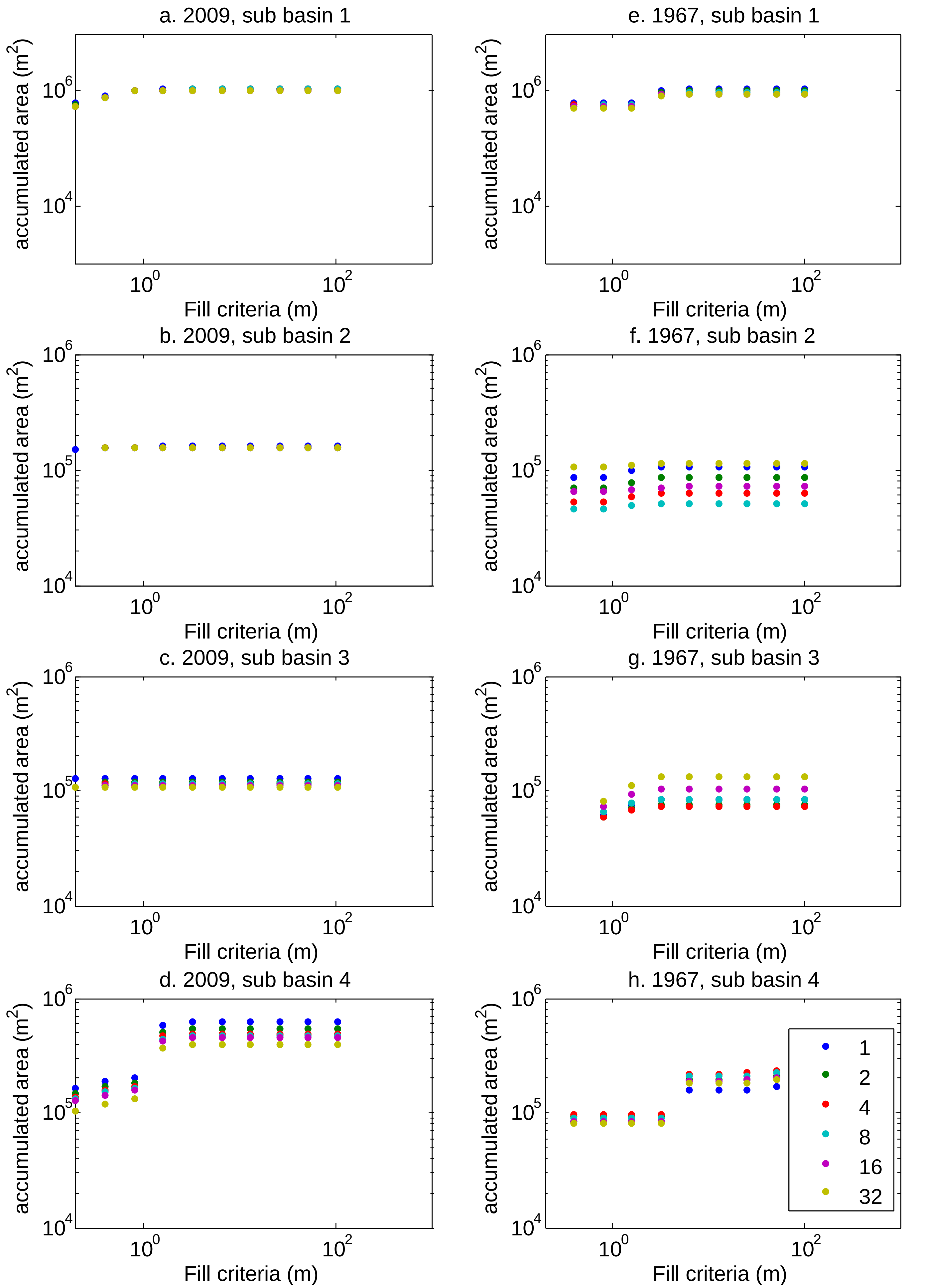

a. 2009, sub basin 1
b. 2009, sub basin 2
c. 2009, sub basin 3
d. 2009, sub basin 4
e. 1967, sub basin 1
f. 1967, sub basin 2
g. 1967, sub basin 3
h. 1967, sub basin 4
accumulated area (m^2)
Fill criteria (m)
10^4
10^5
10^6
10^0
10^2
1
2
4
8
16
32

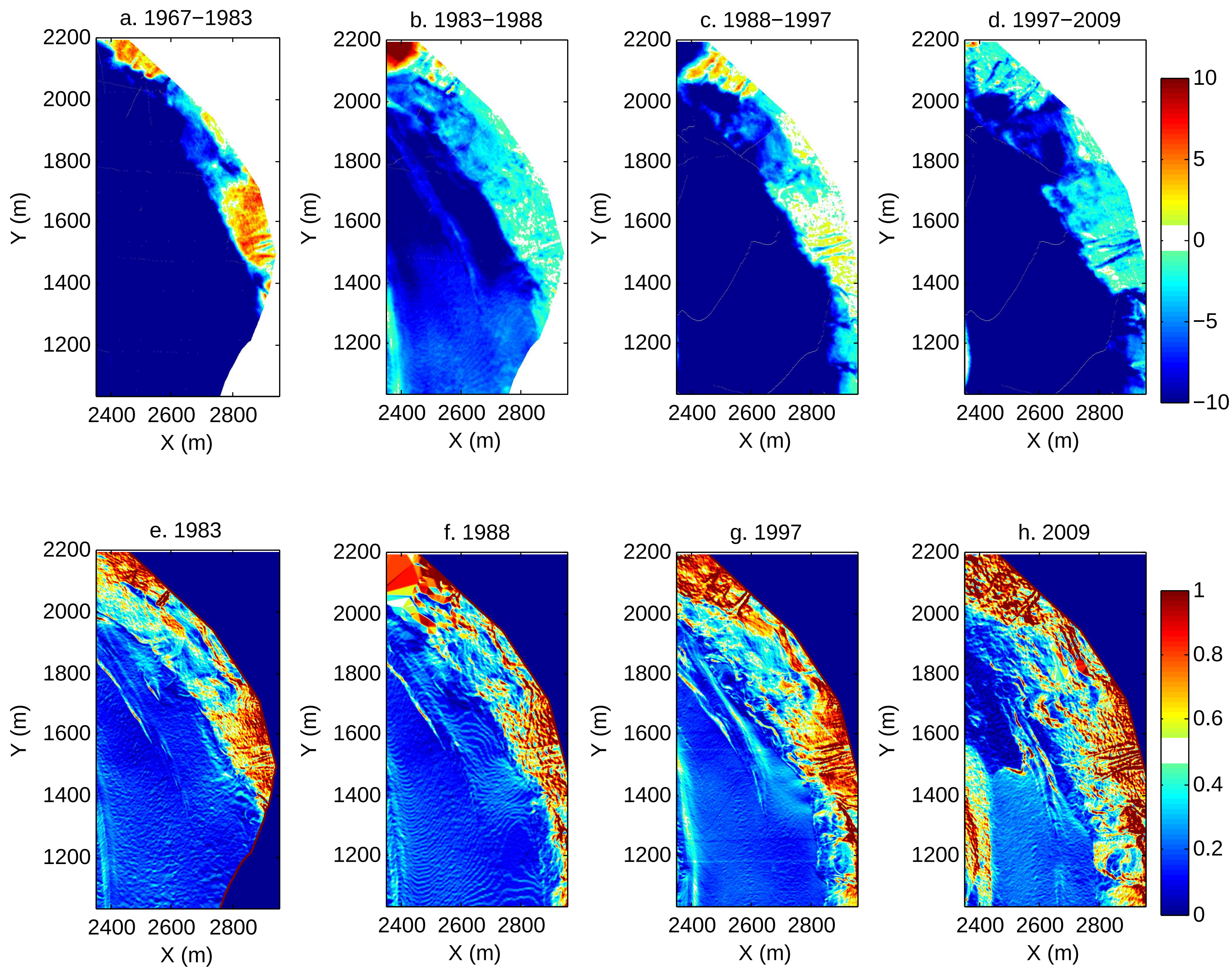

a. 1967−1983
b. 1983−1988
c. 1988−1997
d. 1997−2009
e. 1983
f. 1988
g. 1997
h. 2009
X (m)
Y (m)
2400
2600
2800
1200
1400
1600
1800
2000
2200
10
5
0
−5
−10
1
0.8
0.6
0.4
0.2
0

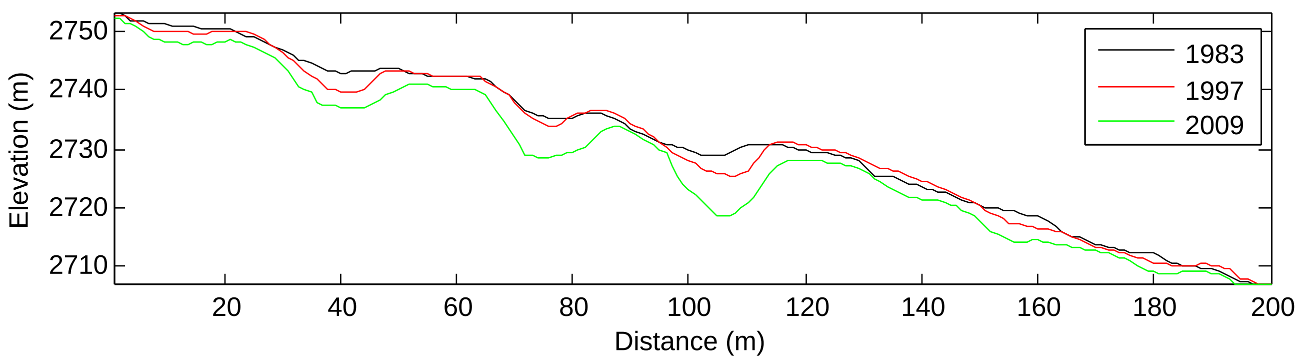

2750
2740
2730
2720
2710
Elevation (m)
20
40
60
80
100
120
140
160
180
200
Distance (m)
1983
1997
2009

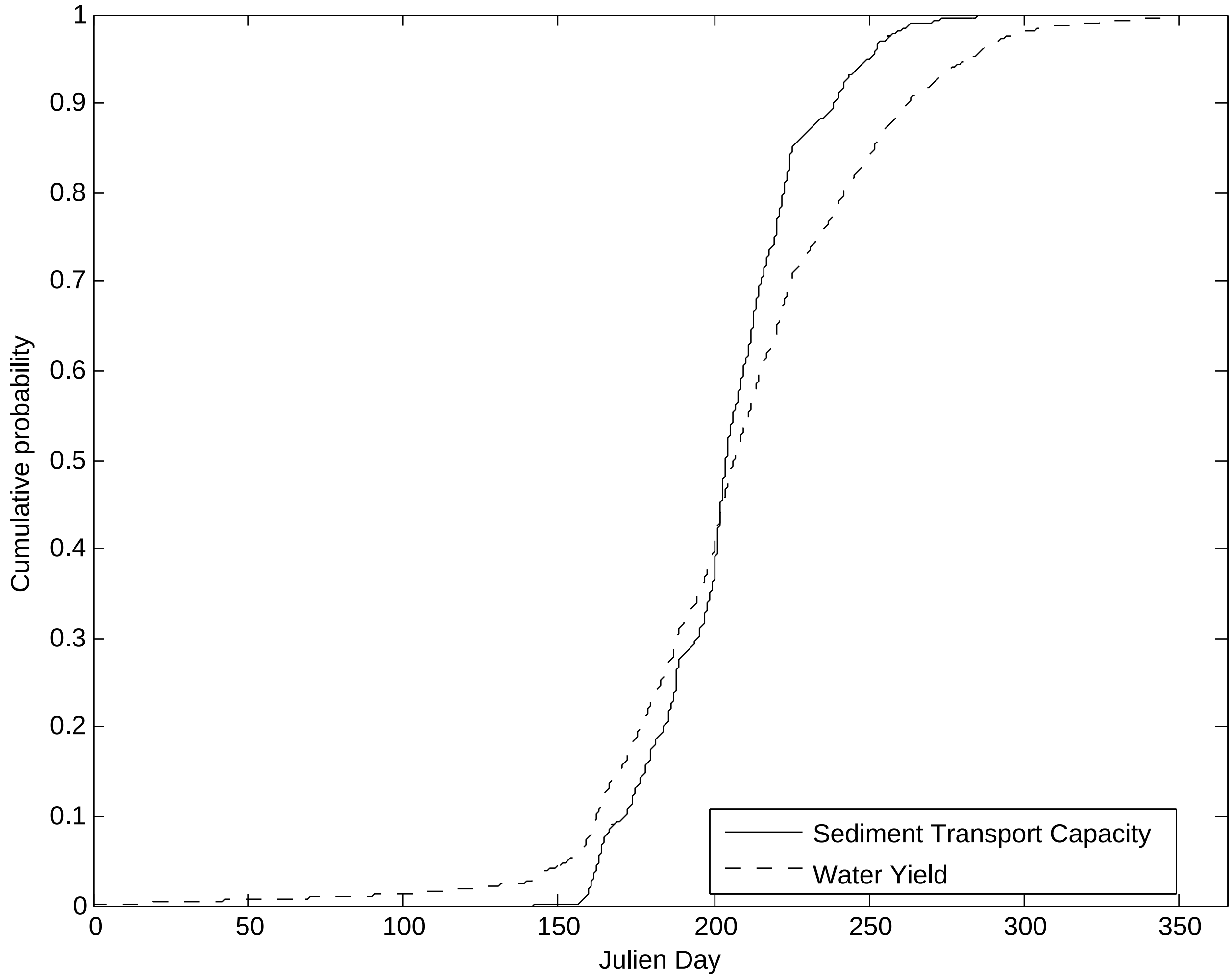

1
0.9
0.8
0.7
0.6
0.5
0.4
0.3
0.2
0.1
0
Cumulative probability
0
50
100
150
200
250
300
350
Julien Day
Sediment Transport Capacity
Water Yield


Sidewalls post recession II
Upper parts of basin contain frozen till
Strong temperature sensitivity
Pre-recession III
1850s moraine
Disconnects east basins
Glacier recession III
Hanging glacier recession
Exposes unworked sediment
Sediment flux limited by capacity to transport sediment
Glacier recession I
Reduces relative glacial disconnection
Pre-recession II
Subglacial streams
High potential transport capacity
But laterally pinned by hydraulic potential
Sidewalls post recession I
Over steepening of side walls
Gullying aids moraine breach
Pre-recession I
Glacier surface sediment transport slow
Relative glacial « disconnection »
Sidewalls post recession III
Melt of ice cored-till and rock fall
Accumulations of well-drained material
Reduces connection at base of sidewalls
Glacier recession II
Transition from subglacial to proglacial stream
Stream can more easily migrate laterally
Access to poorly sorted and more readily transported till increases
Proglacial area post recession I
Rapid expansion of the proglacial zone
Limited by the presence of ice cored moraine
Proglacial area post recession II
Fluvial sorting processes
Reduced rate of downstream transfer

Year	Image scale, x (1: *x*)	Theoretical precision (m)	Global RMSE of bundle adjustment (m)	RMSE X (m)	RMSE Y (m)	RMSE Z (m)	Mean error Z (m)	σ_{2009} (m)	1.96 σ_{2009} (m)
1967	13,700	±0.19	±0.59	±0.83	±0.81	±0.04	0.00	±2.34	±4.59
1977	10,000	±0.14	±0.39	±0.21	±0.23	±0.01	0.00	±0.18	±0.36
1983	12,000	±0.17	±0.35	±0.18	±0.25	±0.08	0.02	±0.21	±0.42
1988	22,200	±0.31	±0.88	±0.42	±0.62	±0.45	0.05	±0.67	±1.32
1997	9,000	±0.13	±0.36	±0.53	±0.45	±0.06	0.01	±0.35	±0.68
2000	9,000	±0.13	±0.37	±0.39	±0.34	±0.07	0.01	±0.34	±0.66
2005	11,900	±0.17	±0.36	±0.33	±0.40	±0.04	0.01	±0.24	±0.47
2009	13,000	±0.18	±0.30	±0.34	±0.24	±0.07	0.02	-	-